



Sustained high rates of morphological evolution during the rise of tetrapods

Tiago R. Simões and Stephanie E. Pierce

The fish-to-tetrapod transition is one of the most iconic events in vertebrate evolution, yet fundamental questions regarding the dynamics of this transition remain unresolved. Here, we use advances in Bayesian morphological clock modelling to reveal the evolutionary dynamics of early tetrapodomorphs (tetrapods and their closest fish relatives). We show that combining osteological and ichnological calibration data results in major shifts on the time of origin of all major groups of tetrapodomorphs (up to 25 million years) and that low rates of net diversification, not fossilization, explain long ghost lineages in the early tetrapodomorph fossil record. Further, our findings reveal extremely low rates of morphological change for most early tetrapodomorphs, indicating widespread stabilizing selection upon their 'fish' morphotype. This pattern was broken only by elpistostegalians (including early tetrapods), which underwent sustained high rates of morphological evolution for ~30 Myr during the deployment of the tetrapod body plan.

Major evolutionary transitions in the history of animal life are marked by widespread phenotypic novelties leading to the development of new body plans and ecological opportunity. Such transitions have been widely recognized in the fossil record and seemingly occur during relatively short spans of geological time^{1–3}. Several studies, especially in the past decade, suggest that phenotypic novelties and innovation during those brief periods of time are characterized by fast rates of morphological change under strong selective pressures, such as during the acquisition of flight during the origin of birds⁴ and several skeletal changes marking the origin of snakes⁵. It has also been long argued that when such transitions have been at the origin of major new clades, high rates of morphological change should be coupled with high taxonomic diversification rates^{1,2}. However, a detailed and quantitative understanding of the evolutionary dynamics behind several important evolution transitions remain largely unknown.

The rise of tetrapods is one of the most iconic and inspiring evolutionary transitions in the vertebrate tree of life as it marks the deep time common ancestry of all 36,000+ species of extant limbed vertebrates (including humans), besides thousands of extinct ones during the last ~370 Myr (refs. ^{6–9}). This transition also characterizes a major environmental shift—from water to land—that is coupled with a hallmark of anatomical and functional changes leading to an entire reorganization of the early vertebrate body plan¹⁰. Despite being studied for decades^{11,12}, several fundamental questions regarding the fish–tetrapod transition remain open, including accurately dating the time of origin of tetrapods¹³, recognizing the closest fish-like relatives to elpistostegalians (the broader group including transitional forms like *Tiktaalik*¹⁴, as well as tetrapods) and the pace at which evolutionary changes led to the origin of the tetrapod body plan¹⁵. Some of the few previous studies addressing those issues, such as the rates of evolution during the origin of tetrapods, have focused on rates of biomechanical change¹⁵ or rates of a single anatomical region (humerus)¹⁶, thus never previously estimating rates of morphological change taking multiple regions of the phenotype into account.

Important to the timing of the origin of tetrapods is the apparent conflict between the osteological and ichnological fossil record. The

oldest known tetrapod body fossils range from ~375 to 372 million years ago (Ma) (refs. ^{17–19}) but the discovery of tetrapod trackways in Poland—the Zachełmie tracks dated at ~390 Ma (refs. ^{20,21})—suggest tetrapods evolved at least 15 Myr earlier. Despite controversy surrounding the precise tracemakers of some other purported early tetrapod tracks, the presence of digits has led to the interpretation of the Zachełmie tracks as the earliest known evidence for tetrapods in the fossil record^{13,20,22}. To complicate matters, the Zachełmie tracks are also older than most other known early tetrapodomorph clade¹³. This mismatch between the osteological and ichnological fossil records has been suggested to be the result of low preservation potential during early tetrapod evolution²² but other untested factors, such as low net diversification rates or high extinction rates, could also explain this pattern²³. Therefore, conciliating the osteological and ichnological evidence for accurately dating the divergence of tetrapods, and tetrapodomorphs in general, has been a cumbersome challenge¹³, with direct implications to detangling the tetrapodomorph phylogeny and putting into question our most basic understanding of the early tetrapod fossil record²².

Here, we examine the time of the origin of tetrapods and the rates of phenotypic (morphological) evolution leading to the acquisition of the tetrapod body plan. We address this by expanding and revising the largest available dataset on early tetrapodomorph evolution²⁴ and analysing it using important advances on relaxed morphological clock Bayesian inference of evolutionary trees (Methods and refs. ^{25–27}). Our main questions include: (1) When did tetrapods and the other major clades of tetrapodomorphs originate? (2) What is the rate of morphological change and diversification dynamics during the deployment of the tetrapod body plan? (3) Are different regions of the phenotype or major clades evolving at similar rates of evolution or varying rates due to distinct selective pressures? Our results indicate that combining osteological and ichnological calibration data yields considerably older divergence times for all the major groups of tetrapodomorphs and significantly lower net diversification rates in the early phase of tetrapodomorph evolution. Further, we find high rates of morphological change sustained for nearly ~30 Myr on the branches leading to tetrapods, consistent

Museum of Comparative Zoology & Department of Organismic and Evolutionary Biology, Harvard University, Cambridge, MA, USA.
✉e-mail: tsimoes@fas.harvard.edu

with several adaptive changes throughout the skeleton during the Devonian period, particularly within the skull.

Results and discussion

The placement of rhizodontids and identifying the closest relatives to tetrapods. Recently, fossil and phylogenetic data have suggested a reconfiguration of the traditional classification of the early tetrapodomorph tree of life²⁸, with rhizodontids (traditionally considered as early-diverging tetrapodomorphs^{14,29,30}) being proposed as the sister group to elpistostegarians instead of tristichopterids (including, for example, the model species *Eusthenopteron*). This alternative hypothesis would have a direct impact on several previous studies that have used *Eusthenopteron* as the starting point for analysis of character evolution at the origin of tetrapods—for example, refs. ^{12,31,32}. Furthermore, such a dramatic reconfiguration of the tetrapodomorph tree would inevitably have a direct impact on estimates for the time of origin of tetrapods and rates of evolution across early tetrapodomorphs.

To further test the phylogenetic placement of rhizodontids and the closest relatives to tetrapods, here we included the recently described oldest known species of tetrapod, *Parmastega*¹⁸, in the largest available dataset of early tetrapodomorphs²⁴. Further, we performed several modifications on this dataset by revising all of the phylogenetic characters that failed to meet basic criteria of character construction (for example, logical or biological redundancy among characters), following standard coding schemes and guidelines for morphological data (for example, refs. ^{33–35}) as detailed in the Methods and Supplementary Information (dataset updates). This altered 15% of the original dataset and resulted in a revised and updated character set used herein for subsequent analyses—revised dataset available online (Data availability).

Nearly all analyses herein using distinct optimality criteria (maximum parsimony and Bayesian inference) and various models for Bayesian inference with relaxed morphological clocks (Methods) recover the traditional relationship of tristichopterids as the closest relatives to elpistostegarians (including tetrapods) (Figs. 1 and 3 and Supplementary Figs. 2–19). The only exceptions were the few initial analyses before the removal of rogue taxa or analyses implementing strong priors conflicting with the phylogenetic signal (Supplementary Figs. 1, 14 and 15). Therefore, our results contrast with recent findings suggesting rhizodontids as the closest lineage to elpistostegarians²⁸. Maximum parsimony and non-clock Bayesian inference analysis depict similar results to ref. ²⁴ in the non-monophyletic of tristichopterids at the base of the branch leading to early elpistostegarians (Supplementary Figs. 2 and 3). However, all relaxed morphological clock analyses find tristichopterids as the sister clade to elpistostegarians, thus consistent with the classical hypotheses of early tetrapodomorph relationships^{14,29,30} (Supplementary Information). Rhizodontids are consistently placed among early tetrapodomorphs, either as the earliest clade relative to all other tetrapodomorphs or still part of the early tetrapodomorph radiation but as the sister clade to osteolepidids (Figs. 1 and 3 and Supplementary Figs. 2–19). *Tiktaalik* was consistently found further crownward and as the closest sister group to tetrapods instead of *Elpistostege*, thus differing from the most recent phylogenetic analysis of tetrapodomorphs²⁴ but similarly to one previous Bayesian inference analysis²⁸. Further, the newly described *Parmastega* was recovered as the earliest deriving tetrapod, consistent with prior phylogenetic analysis of a more tetrapod-focused dataset¹⁸.

Integrating osteological and ichnological calibration data pushes back diversification times for tetrapodomorphs. We tested the differential impact on tree topology, divergence times and other macroevolutionary parameters from various model assumptions for Bayesian morphological clock analyses, including: distinct clock models (uncorrelated and autocorrelated clocks); tree models (that

is, diversification parameters constant throughout the tree—fossilized birth-death process (FBD) versus diversification parameters variable across time bins—skyline FBD process (SFBD)); and sampling strategies (allowing versus not allowing for ancestors in the tree). These distinct models were tested across different programs (MrBayes and BEAST2)^{36,37} for potential variations in the results due to software implementation—Methods).

Using the fossil tips as the exclusive source of age calibration (as in typical tip-dated Bayesian morphological clock inference), all results indicate the time for the split between dipnomorphans and tetrapodomorphs to be at ~416–420 Ma (Fig. 1a and Supplementary Figs. 5, 7, 9, 11 and 13). This result is consistent with previous findings in a broader gnathostome phylogeny using similar parameter-rich evolutionary models³⁸. Additionally, we find the divergence of the tetrapod branch from their most recent common ancestor with *Tiktaalik* has a median estimate between 373 and 378 Ma among all clock and tree models (Fig. 1a and Supplementary Figs. 5, 7, 9, 11 and 13). This estimate is at least 12 Myr younger than the Zachełmie tetrapod tracks^{20,21}, indicating that no analytical procedures using state-of-the-art tip-dating approaches are able to retrieve a time-tree that conciliates the osteological and ichnological evidence.

To account for the limitation above, we integrated fossil tip ages with the age of the Zachełmie tracks in the form of a single node age calibration informing the minimum age for the divergence of tetrapods from other tetrapodomorphs. Following this procedure, the estimated origin for the Tetrapoda branch shifts considerably into the past, although only slightly older than the Zachełmie tracks, at 390.34 Ma (upper 95% highest posterior density interval (HPD) = 391.5 Ma) (Fig. 1b, Extended Data Fig. 3 and Supplementary Figs. 17 and 19). On the other hand, the median age for the most recent common ancestor of all known tetrapods is 372.9 Ma (95% HPD = 372–375.1 Ma), therefore implying a long ghost lineage on the tetrapod stem of ~18 Myr. A similar long branch is observed on other deep branches, such as on the elpistostegalian stem, with the divergence between elpistostegarians from other tetrapodomorphs estimated at 415 Ma (95% HPD = 408–423.2 Ma).

The inclusion of a node calibration for tetrapods that is much older than any tip calibration is expected to result in older divergence times for several parent and daughter nodes of the calibrated node. This is expected on the basis of our current understanding of node calibration approaches, in which only a few nodes are necessary to calibrate the entire tree and can provide important complementary calibrations to tip-dating (for example, ref. ³⁹). However, we surprisingly found that this single node calibration also had a substantial impact on several other nodes, including all sister clades to elpistostegarians that do not represent immediate ancestor or descendant nodes to the calibrated node (for example, nodes on the early divergence of rhizodontids and osteolepidids—Fig. 1). Importantly, node dating is traditionally performed on the basis of the age of the oldest known osteological fossil of a clade but, as in the case of early tetrapodomorphs, the use of the osteological record only would not suffice to substantially shift divergence times to match the age of the oldest known tetrapod trackways. Therefore, even though reasonable ichnological evidence for a precise node calibration can be extremely rare, we highlight its potential relevance and demonstrate its power to complement tip dating and correct underestimated divergence times throughout the entire tree, even if based on a single node calibration.

Low net diversification generates long ghost lineages in early tetrapodomorph evolution. Long ghost lineages can be the result of low preservation potential (parameterized here under the fossil sampling probability of the FBD process), as previously suggested to explain the apparent lack of fossils in early tetrapodomorph evolution²². However, it may also be a result of low net diversification

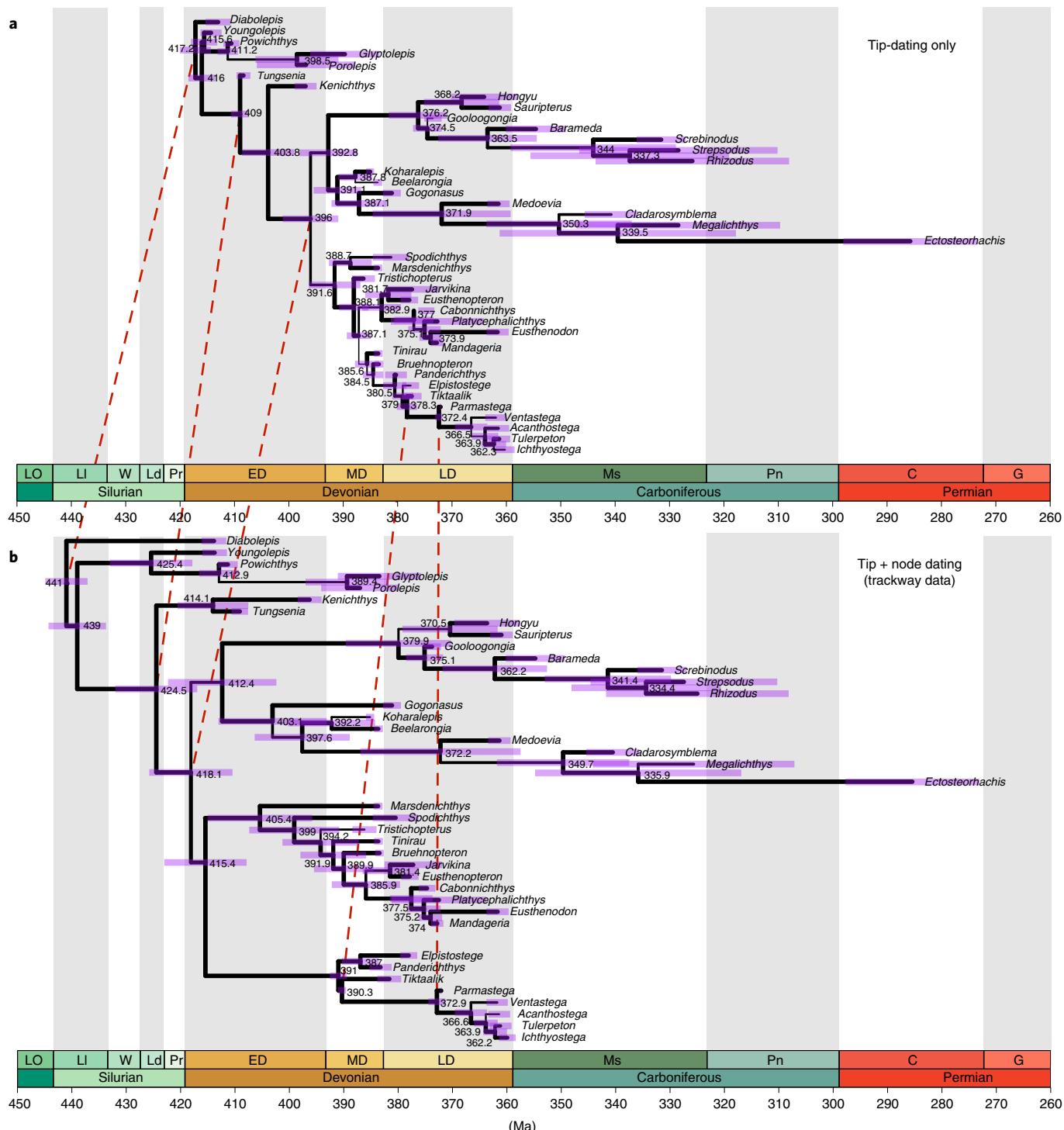


Fig. 1 | Comparison of evolutionary trees and divergence times for the major groups of tetrapodomorphs using distinct tree calibration strategies.

a, Maximum compatible tree from the main tip-dating-only analysis using the SFBD tree model (Model 8; Extended Data Fig. 3 and Supplementary Figs. 12 and 13). **b**, Results from the main tip + node dating (including trackway age data) analysis using the SFBD tree model with a single clock partition (Model 10; Extended Data Fig. 3 and Supplementary Figs. 16, 17 and 29). Node values represent median ages; purple error bars represent the 95% highest posterior density (HPD) intervals; branch thickness proportional to posterior probabilities; dotted lines connect equivalent notes between trees. Accounting for both osteological and ichnological evidence pushes back the time of origin of tetrapods and other major clades between ~10 and ~23 Ma. Results from **b** remain largely unaltered using partitioned morphological clocks. C, Cisuralian; ED, Early Devonian; G, Guadalupian; LD, Late Devonian; LI, Llandovery; Ld, Ludlow; LO, Late Ordovician; MD, Middle Devonian; Ms, Mississippian; Pn, Pennsylvanian; Pr, Pridoli; W, Wenlock.

rates, high extinction rates²³ or low background evolutionary rates (for example, base of the clock rate in relaxed clock analyses)²⁷. Using the SFBD tree model with and without ichnological data

(Methods) we assessed which aspects of early tetrapodomorph evolution need to be reconsidered given the more ancient divergence times introduced by the Zachełmie tracks.

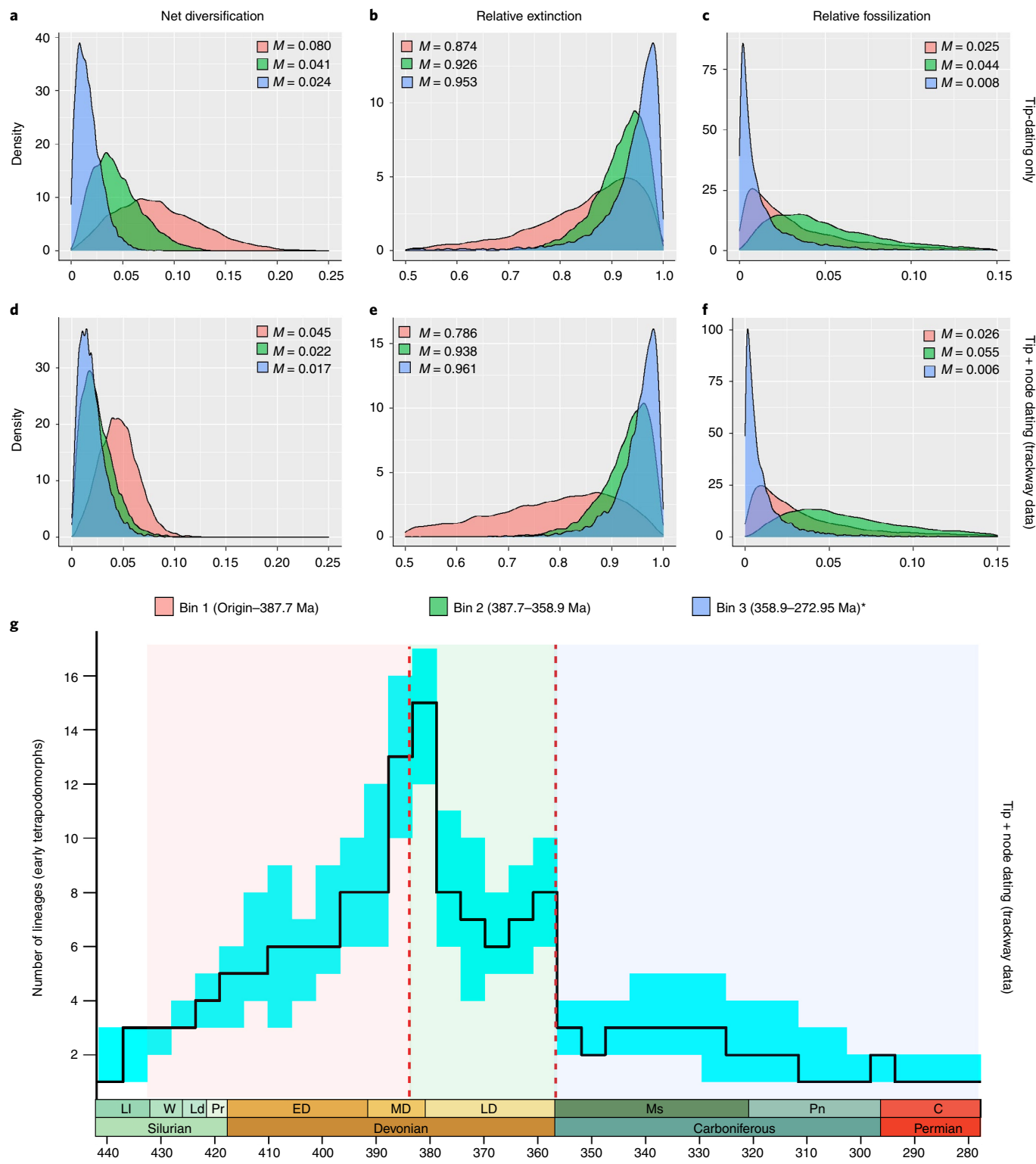


Fig. 2 | Shifts in diversification parameter estimates from the FBD process and LTT across time bins. **a–c**, Kernel densities from main tip-dating-only analysis (Model 8). **a**, Net diversification. **b**, Relative extinction. **c**, Relative fossilization. **d–f**, Kernel densities after incorporating the age of the Zachelmie tracks (Model 10). **d**, Net diversification. **e**, Relative extinction. **f**, Relative fossilization. **g**, LTT plot, black line represents median values whereas shaded area (cyan) represents the 95% confidence interval taken from a random subsample (2,000 trees) from all posterior trees. Panels **d–g** are based on the main tip + node dating analysis (including trackway age data). Net diversification nearly halves for the first and second time bins under the tip + node (trackway data) divergence times. Relative extinction values also decrease but to a lower extent (-10%) for bin 1, whereas median relative fossilization remains similar between analyses (Extended Data Fig. 1). Further, the tip + node (trackway data) diversification scenario suggests a less drastic reduction in net diversification between time bins 1 and 2 (**d**) during early tetrapodomorph evolution. *Note: Time bin 3 only includes early tetrapodomorphs; later evolving tetrapods are not represented and so this part of the LTT plot should not be interpreted literally (see text for details). M, median.

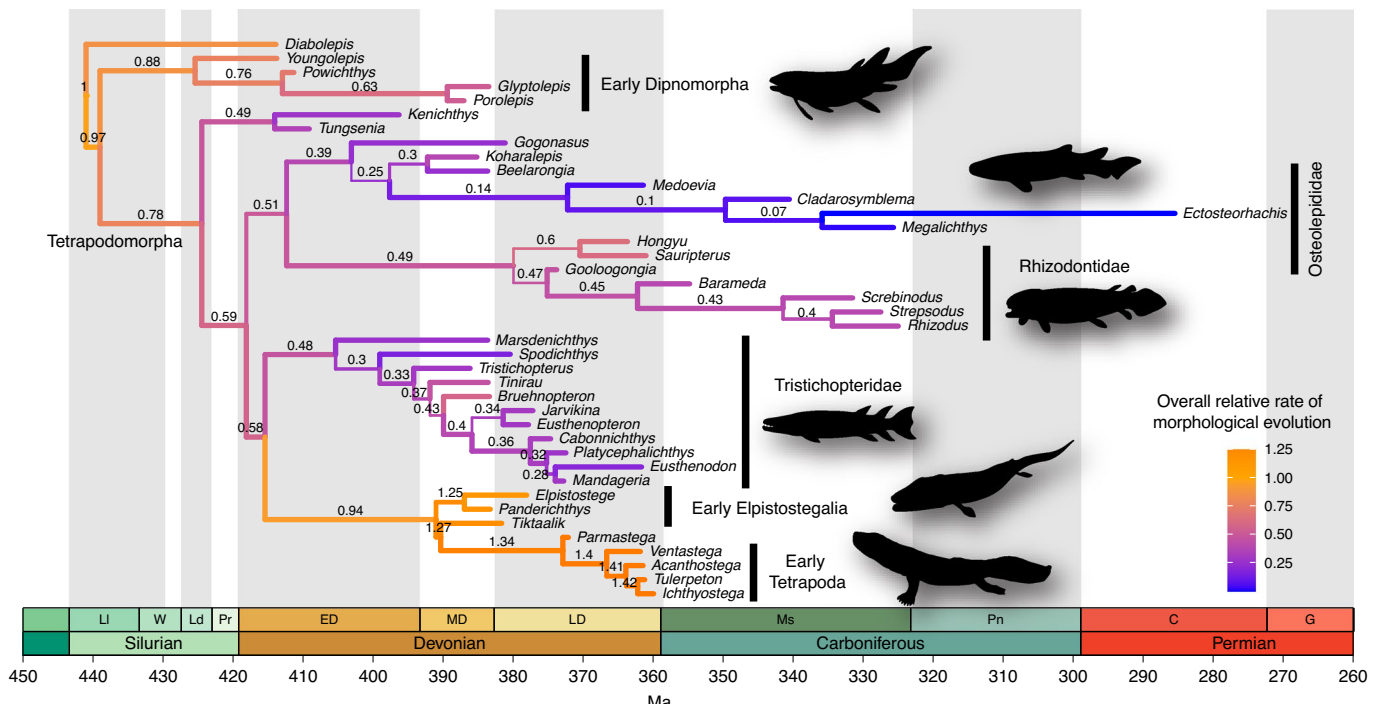


Fig. 3 | Relative overall rates of morphological evolution in early tetrapodomorphs. Median relative rates of morphological evolution obtained from the main tip + node dating analysis (including trackway age data) using a single morphological clock partition (Model 10). Relative rates of evolution increase in elpistostegarians, and even further in the transition to the earliest tetrapods, across all measures (Extended Data Fig. 4).

Results using tip-only dating indicate an overall low value for net diversification and relative fossilization along with a high relative extinction for early tetrapodomorphs (Fig. 2, Supplementary Figs. 21–23 and Supplementary Table 5). These are expected considering the early diversification of tetrapodomorphs into four major clades during the Devonian but with most of them going extinct during the Carboniferous (except, for example, tetrapods). Even in the case of tetrapods, these remain low in diversity during most of the Early Carboniferous (Mississippian) period—the so-called ‘Romer’s gap’—and increase in diversity and abundance only from the Late Carboniferous (Pennsylvanian) period onwards^{12,40}. Importantly, analyses accounting for the trackway age data (Fig. 2c–e, Supplementary Figs. 25–27 and Supplementary Tables 6) recover net diversification estimates that are 50% lower than estimates from the tip-only dating analysis between the origin of tetrapodomorphs until the end of the Devonian (358.9 Ma) (Fig. 2, Extended Data Fig. 1 and Supplementary Tables 7–10). Relative extinction values slightly decrease between the origin of tetrapodomorphs and 387 Ma but only by 10%, whereas median rates are very similar for the subsequent time bins. Interestingly, relative fossilization rates are similar between analyses with and without accounting for the trackway age data, suggesting that a change in the fossilization rate is not responsible for the long ghost lineages in early tetrapodomorph evolution.

To visualize the combined effect of the parameters above on the total number of lineages available across time during early tetrapodomorph evolution, we produced a lineage through time (LTT) plot (Fig. 2g) with the phytools R package⁴¹. The result indicates a sustained increase in the total number of lineages between the Silurian and the Middle Devonian periods, reaching its peak at ~380 Ma at the beginning of the Late Devonian. Diversity then decreases and stabilizes at intermediate levels throughout the remainder of the Late Devonian. Finally, diversity sharply decreases to extremely low values at the onset of the Early Carboniferous. The latter decline is coincident with the end-Devonian mass extinction but it is

important to note that the current dataset does not include later evolving tetrapods and so the LTT results should not be interpreted literally, although they do reflect the general decreasing trend in tetrapodomorph diversity into the Early Carboniferous, a pattern often associated with Romer’s gap^{12,40}. The increase in diversity, followed by stabilization and decline as found in the LTT plot reflects well the sharp reduction in net diversification detected across time bins 1 to 3 (Fig. 2d–f). Furthermore, the absolute number of lineages in the LTT plot is always low (almost always <10), suggesting a low number of species occurring at any given time, including the early phase of tetrapodomorph radiation (440–387 Ma) when net diversification is at its highest but severely bounded by high relative extinction rates.

The combination of these results thus indicates that long ghost lineages in the early evolutionary history of tetrapodomorphs are not driven by fossilization parameters but most likely to be driven by low net diversification rates. A significantly lower net diversification means that fewer species are available at any given time between 441 and 358 Ma (Fig. 2g) and, therefore, fewer species will be available to be preserved as fossils—even if the fossil preservation rate itself is kept nearly constant. The overall effect is much longer branch durations on the early evolution of tetrapodomorphs and older divergence times.

Finally, upon a survey of depositional environments (Methods), we found that early tetrapodomorph specimens have been found in all major continental/terrestrial aquatic environments, including saltwater (for example, nearshore and offshore marine; total = 30.77%), freshwater (for example, fluvial and lacustrine; total = 56.4%) and brackish water (for example, estuary and lagoonal; total = 12.82%)—Extended Data Fig. 8 and Supplementary Table 11. As with most extant species of fish, the environments with higher specimen sampling are freshwater environments derived from rivers and lakes. This further suggests no detectable large-scale preservation biases towards specific depositional environments in their fossil record.

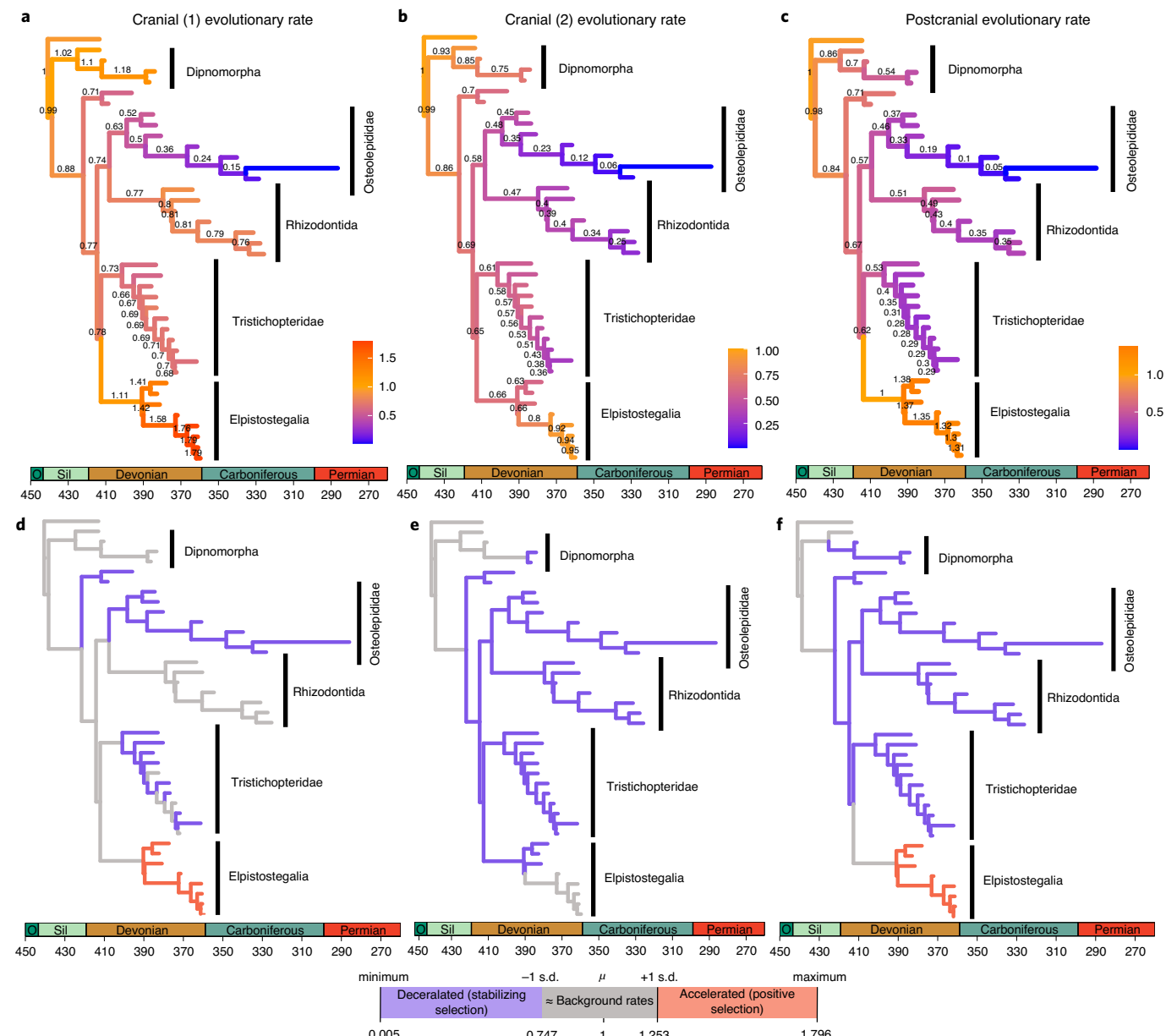


Fig. 4 | Relative rates of evolution and inferred mode of selection across subdivisions of the phenotype in early tetrapodomorphs. **a–c**, Relative rates of morphological evolution using tip + node dating analysis (including trackway age data) using the SFBD tree model under PRMC (Model 11). **a**, Cranial (1) evolutionary rates. **b**, Cranial (2) evolutionary rates. **c**, Postcranial evolutionary rates. Scale bars and branch colours in **a–c** indicate relative rates of morphological change and x axis values represent time (Ma). **d–f**, Branch colours represent significantly accelerated rates (orange) indicating positive selection and decelerated rates (purple) indicating stabilizing selection, whereas grey branches have rates not significantly different from the mean background rate. Bottom scale bar indicates thresholds between significantly different relative rate values plotted on **d–f**. **d**, Cranial (1) significantly accelerated and decelerated branches. **e**, Cranial (2) significantly accelerated and decelerated branches. **f**, Postcranial significantly accelerated and decelerated branches. Widespread decelerating rates in all skeletal regions across most lineages suggest widespread stabilizing selection in tetrapodomorphs retaining a ‘fish-like’ body plan. Accelerated rates in the largest cranial partition (Cranial 1) and in the postcranium of some early elpistostegalians and in early tetrapods suggest significant positive selection towards the acquisition of the tetrapod body plan (Extended Data Figs. 5 and 6).

Sustained high rates of morphological evolution leading up to tetrapods. Divergence times and rates of evolution are interdependent parameters and, therefore, older divergence times should result in slower rates of character change²⁷. As expected, the base of the clock rate in the analysis accounting for the trackway data was reduced to a third of the rate inferred from the tip-only analysis (Extended Data Fig. 2 and Supplementary Figs. 20 and 24). However, elpistostegalians display the highest rates of morphological evolution among all tetrapodomorphs, for analyses with

and without trackway data (Extended Data Fig. 4a). In the analysis accounting for the trackways, early tetrapods have the highest rates among elpistostegalians and all other tetrapodomorphs, reaching up to 42% above background rates of evolution (Fig. 3 and Extended Data Fig. 4b). This increase is consistent with previous theory and findings that the origin of new body plans should be characterized by high rates of morphological evolution—for example, refs. ^{1,4,5}. On the opposite end of the spectrum, osteolepidids have the lowest relative rates of morphological evolution

among all tetrapodomorphs, between only 7 and 25% of the background rates (Fig. 3).

To estimate rates of morphological change across distinct phenotypic regions (for example, cranial versus postcranial) independently, we used a new method proposed here to automatically detect morphological regions for partitioned relaxed morphological clock analyses (PRMC; Methods). We find rates of cranial evolution among tetrapodomorphs are significantly higher than rates of postcranial evolution, with rates among most cranial characters (Cranial 1 partition) evolving twice as fast as postcranial characters among rhizodontids, osteolepidids and tristichopterids (Figs. 4a and 5a,b, Extended Data Fig. 5 and Supplementary Tables 12 and 13). In sharp contrast, elpistostegalians (including early tetrapods) underwent relatively fast rates of both cranial and postcranial evolution, with the fastest skull rates (79% above background rates) being only about one-third higher than postcranial rates (31% above background rates) for the same evolutionary branches (Figs. 4c and 5d). In comparison, other branches had cranial rates about two times faster than the rates of postcranial evolution (Supplementary Table 13). When compared across clades, cranial rates of evolution in elpistostegalians are on average more than two times faster than cranial rates in other tetrapodomorphs (up to eight times faster in early tetrapods compared to osteolepidids), whereas postcranial rates in elpistostegalians are on average more than four times faster than postcranial rates in other early tetrapodomorph clades (up to 12 times faster in early tetrapods compared to osteolepidids) (Fig. 4a–c and Supplementary Table 13).

Widespread stabilizing selection in tetrapodomorphs broken by adaptive changes on the construction of the tetrapod body plan. Adaptive change is considered to be a major driver of morphological evolution in deep time scales and theory suggests accelerating relative rates of phenotypic change indicate positive selection whereas decelerating rates indicate stasis or stabilizing selection⁴². Therefore, detecting significant changes on rates of evolution across branches of evolutionary trees enables an indirect measure of strength of natural selection, as similarly performed in molecular evolution^{42,43}. Here, we expand on the existing approach of using phylogenetic comparative methods to detect rates of evolution and the strength of selection using morphological data⁴² to PRMC analyses. We use phylogenetically determined rates of evolution to infer the rate scalar ratio (r) and the uncertainty around the mean taken from the posterior to detect evolutionary branches undergoing significantly accelerated/decelerated morphological change—the basis for detecting positive versus stabilizing selection (Methods).

Our results on early tetrapodomorphs reveal the only detectable instance of positive selection was during the evolution of elpistostegalians, especially at the origin of tetrapods. Positive selection is observed for most cranial characters (Cranial 1 partition here) and all postcranial characters (Fig. 4d–f and Extended Data Fig. 6), although less strongly in the latter than for cranial characters. On the other hand, the strongly decelerating rates of morphological evolution detected throughout the skeleton for all other early tetrapodomorph clades suggest stabilizing selection on many of

those lineages for the maintenance of their ‘fish-like’ body plan (Fig. 4d–f). Specifically for cranial characters we detect stabilizing selection in two clades (tristichopterids and osteolepidids), whereas

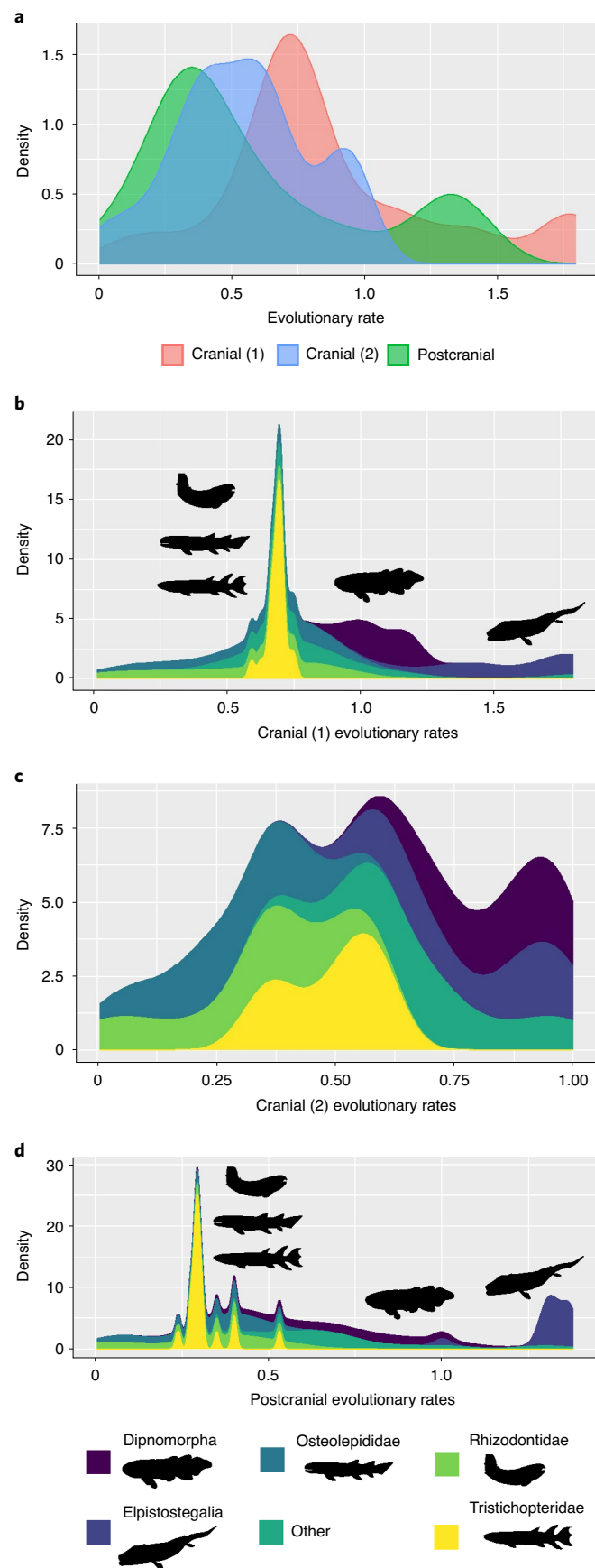


Fig. 5 | Distribution of relative rates of evolution for each morphological partition across tetrapodomorphs. **a**, Kernel densities of evolutionary rates for each morphological partition for all clades. **b**, Stacked kernel densities for rates of evolution for the larger cranial partition (1) across clades. **c**, Stacked kernel densities for rates of evolution for the smaller cranial partition (2) across clades. **d**, Stacked kernel densities for rates of evolution for the postcranial partition across clades. Despite variation across distinct skeletal regions, relative rates of morphological evolution in elpistostegalians (especially driven by early tetrapods) are distinctively higher relative to their closest ‘fish-like’ tetrapodomorph relatives.

in early dipnomorphans and rhizodontids the rate of evolution of most cranial characters are at either background levels (Cranial 1) or undergoing stabilizing selection (Cranial 2)—Fig. 4d,e. In the postcranial partition, all clades outside elpistostegaliens undergo widespread stabilizing selection (Fig. 4f), which is broken only by elpistostegaliens.

Our findings thus indicate a stronger adaptive role of cranial features during the initial acquisition of the tetrapod body plan in the Devonian relative to the postcranium. Cranial character changes observed among early tetrapods (responsible for the highest rates of evolution among tetrapodomorphs) include consolidating cranial bones (for example, reduction in the number of elements, such as nasals and loss of intertemporals), modifications to the braincase (for example, reduction in length of parasphenoid) and extensive adaptations related to feeding (loss of the intracranial joint, expansion of parasymphysial dental plate, complete loss of fangs on ectopterygoids). Those in the postcranium are mainly related to further development of a distinct pectoral region with greater area for muscle attachment (for example, anocleithrum without interior overlap area; kite-shaped interclavicle)^{12,13}. Collectively, these results indicate elpistostegaliens and, especially early tetrapods, were able to rapidly specialize through a series of positively selected modifications in their skull (and shoulder) anatomy related to feeding and food procurement, such as the transformation from a suction-based mode of prey capture to biting^{44,45} and substantial increase in visual range by increasing the size of their orbits⁴⁶. It is possible, however, that stronger adaptive selection on the postcranium relative to cranial features happened later in tetrapod evolution, during the Permo-Carboniferous period, as tetrapods started to more fully exploit the terrestrial environment. Indeed, recent evidence indicates that the earliest tetrapods were not optimized for limb-based locomotion and that further adaptations to the postcranial musculoskeletal system were required to fully exploit the terrestrial environment^{32,47,48}. Our findings based on evolutionary rates thus support recently accumulating biomechanical and functional evidence^{32,45,46,48} suggesting the fundamental role of cranial adaptations during the fish–tetrapod transition preceded key adaptations of the postcranial skeleton.

Conclusions

Our findings highlight new fundamental aspects regarding the rise of tetrapods. Using recently developed relaxed morphological clock model implementations, we find that only by combining age calibrations from the osteological and the ichnological record is it possible to recover estimates for the origin of tetrapods and other tetrapodomorphs that are in accordance with the oldest occurrence of the group (the Zachełmie tracks in Poland). These age estimates have a strong and direct impact on inferring rates of morphological evolution and diversification dynamics in tetrapodomorphs. Specifically, accounting for the ichnological fossil record results in long ghost lineages for all major tetrapodomorph clades and significantly lower net diversification rates during the early evolution of tetrapodomorphs in the Devonian period—rather than lower fossilization rates as previously suspected²². Therefore, our results indicate that both osteological and ichnological fossil calibration data should be considered (where appropriate) in future investigations of divergence times (for example, using molecular and/or morphological clock approaches) during the origin of major clades.

Using our newly proposed automatic partitioning method of morphological characters for PRMC analyses and extending approaches to detect the strength of natural selection on the phenotype⁴² to clock-based Bayesian inference, we bring morphological phylogenetics closer to standard practices in molecular phylogenetics. As a result, we find that the evolutionary changes throughout the skeleton of some elpistostegaliens and early tetrapods were driven by positive adaptive selection (stronger in the skull relative to the

postcranium) during the deployment of the tetrapod body plan and characterized by a series of evolutionary bursts for ~30 Myr between the Middle and Late Devonian period. The highest rates of both cranial and postcranial evolution are observed in the early radiation of tetrapods, on the branches separating the first known species of tetrapod (*Parmastega*) and *Ichthyostega* + *Tulerpeton*, consistent with positive adaptive change during a time span of only ~6 Myr (Fig. 3a). The fastest rates are concentrated on the skull, including several adaptations for feeding, suggesting that as primary evolutionary driver towards the acquisition of the tetrapod body plan. All other early tetrapodomorph clades are marked by widespread stabilizing selection towards maintaining their extremely well-adapted ‘fish-like’ body plan for life under water.

Despite the low known taxonomic diversity of early tetrapods during the Late Devonian^{12,40} and extremely low rates of net diversification (Fig. 2), the rise of tetrapods is marked by much faster rates of phenotypic change compared to contemporaneous and closely related tetrapodomorph lineages. This provides a strong example of the decoupling between periods of taxonomic radiation (such as during adaptive radiations) from the time of origin of major clades—usually characterized by fast phenotypic change—such as detected here and more recently during the early evolution of lepidosaurs in the Mesozoic era⁵ and the radiation of horses during the Neogene period⁴⁹. This taxonomic-character rate divide may thus be more common than previously assumed by traditional evolutionary theory^{1,2} and may, instead, represent a more widespread feature of macroevolution.

Methods

For additional details of the methodological procedures, see Supplementary Methods and Table 1.

Morphological dataset. We used a dataset representing the broadest sampling of early tetrapodomorphs inclusive of the earliest tetrapods²⁴. This dataset contained 42 taxa and 205 characters with even sampling of taxa and characters covering all the major clades of early tetrapodomorphs and representing a compilation of characters and taxa from various previous datasets—for example, Daeschler et al.¹⁴, Zhu et al.²⁸ and Swartz³⁰—to which we performed further additions and corrections (see below). Our choice for an early tetrapodomorph dataset is based on our intent to assess the sister group relationship among early tetrapodomorphs and on recent evidence indicating that the most accurate posterior parameter estimates from Bayesian relaxed clock analyses come from shallow/most recently diverged nodes, as those are more robust to model misspecifications in both empirical and simulated datasets^{27,50}. Therefore, parameters such as the divergence time of tetrapods are better assessed in datasets where early tetrapods represent shallow nodes (as in ref. ²⁴) instead of deep nodes in the tree (closer to the root).

To this dataset, we added the oldest known tetrapod species, *Parmastega*¹⁸, which is key to understanding both the timing of and the morphological changes associated with the fish–tetrapod transition, with additional taxon scoring corrections. Importantly, we revised the dataset to remove or recode morphological characters that were logically or biologically dependent on each other, along with other inconsistent character constructions, following standard coding schemes and guidelines for morphological data (for example, refs. ^{33–35}) as detailed in Supplementary Information (dataset updates). A total of 27 characters were removed and seven characters had to be recoded (three split into two characters), altering 15% of the original dataset and resulting in a revised and updated dataset used herein for subsequent analyses—revised dataset available online (Data availability). The final dataset included 43 taxa and 178 characters, with a proportion of cranial and postcranial characters of ~2:1, or 33% of postcranial characters, which is similar to most other vertebrate morphological datasets we are aware of. We note that here we count characters related to the pectoral girdle of tetrapods as part of our cranial set of characters, as those elements are associated with the skull of ‘fish-like’ tetrapodomorphs that constitute most of the taxon sampling here (see more below on character partitioning). If we were to include pectoral elements among postcranial characters, the latter would correspond to an even higher proportion (44%) of all sampled characters.

In initial analyses, we found low support and weak leaf stability for the placement of three taxa with high levels of missing data (*Gyroptychius*, *Canowindra* and *Osteolepis*) that fluctuate between rhizodontids, osteolepidids or a clade comprised by the former two (Supplementary Figs. 3–11). Those wildcards were removed from subsequent focal analyses following general recommendations for improvement of phylogenetic accuracy^{51,52}, generating evolutionary trees with higher support that were used for extracting macroevolutionary parameters.

Table 1 | Model combinations tested for the relaxed morphological clock Bayesian inference of the tetrapodomorph dataset

Model	Rogue taxa removed	Topology constraint	Clock model		Tree model			Program
			Clock partitions	Clock type	Sampling	FBD model	Calibration	
Initial analyses								
1	No	No	One	Unco(Ln)	SA	FBD	Tips	BEAST2
2	No	No	One	Unco(Ln)	nosa	FBD	Tips	BEAST2
3	No	No	One	Unco(IGR)	nosa	FBD	Tips	MrBayes
4	No	No	One	Auto(TK02)	nosa	FBD	Tips	MrBayes
5 ^a	No	No	One	Unco(IGR)	SA	FBD	Tips	MrBayes
6 ^a	No	No	One	Auto(TK02)	SA	FBD	Tips	MrBayes
Focal analyses								
7	Yes	No	One	Auto(TK02)	nosa	FBD	Tips	MrBayes
8 ^b	Yes	No	One	Auto(TK02)	nosa	SFBD	Tips	MrBayes
9	Yes	No	One	Auto(TK02)	nosa	SFBD	Tips + node	MrBayes
10 ^b	Yes	Yes	One	Auto(TK02)	nosa	SFBD	Tips + node	MrBayes
11 ^b	Yes	Yes	Three	Auto(TK02)	nosa	SFBD	Tips + node	MrBayes

See Methods and Supplementary Methods for further details on each analytical procedure. ^aAnalyses with poor diagnostic values. ^bBest-performing model combinations for analyses using tip-only calibrations (Model 8) and tip + node calibrations (including trackway data) using single (Model 10) and partitioned (Model 11) morphological clocks.

Phylogenetic and macroevolutionary analyses. We tested the revised dataset on early tetrapodomorphs using maximum parsimony, non-clock Bayesian inference and relaxed morphological clock Bayesian inference (the data parameters are available in Supplementary Information). Below we provide a summary of our relaxed morphological clock approach and its usage for macroevolutionary inference.

Relaxed clock Bayesian inference approaches for the joint estimate of the best tree topology, divergence times and evolutionary rates, among other parameters, is an important approach towards an integrative inference of evolutionary trees with macroevolutionary parameters using molecular data, morphological data or both^{5,53}. This was especially promoted by advances on tree modelling, such as the FBD tree model and its skyline variant SFBD, which allows speciation, extinction and fossilization parameters to vary across time bins^{26,54,55}. Those model developments can provide accurate estimates of macroevolutionary parameters, including net diversification, turnover and fossil sampling rates^{50,56}, while relaxed clocks can provide reliable rate estimates even with taxon sampling limited to nine species only⁵⁷. In recent years, this approach has been especially useful on assessing the dynamics of deep time evolutionary patterns in fully extinct lineages, which were previously limited to a posteriori estimates of macroevolutionary parameters often based on a fixed tree topology, usually derived from maximum parsimony. As a result, many important studies have been able to infer divergence times and evolutionary rates using morphological clocks for various extinct lineages representing datasets of various compositions and sizes^{38,58–60}.

Character and clock models. We implemented those advances here to uncover the deep time evolutionary dynamics of early tetrapodomorphs. To account for potential differences among programs and a wider range of model choices, we used both MrBayes³⁶ and BEAST2³⁷. We assessed the fit of the different model combinations to our data using the stepping-stone sampling strategy to assess the marginal model likelihoods⁶¹ and calculated Bayes factors (BFs)⁶²—50 steps for 100 million generations. For the model of character evolution, we tested for the best-fitting probability distribution (gamma or lognormal) to model among character rate variation (ACRV) in our dataset, as well as the best strategy to model character state frequencies. For clock models, we tested between two distinct uncorrelated clocks— independent gamma rate (IGR) (MrBayes), and the uncorrelated lognormal clock (Unco(Ln))—and also one autocorrelated relaxed clock (TK02) (MrBayes).

Additionally, we tested for the impact of morphological clock partitioning. Specifically, we conducted analyses in which all morphological characters are treated as a single partition and a set of analyses in which all characters were subdivided into morphological partitions following an automatic partitioning approach described here (see below). For the latter, we assigned a separate morphological clock to each partition, thus allowing us to obtain separate estimates of character evolution for each partition (for example, cranial versus postcranial partitions). This strategy is especially relevant to address some of the important questions on early tetrapodomorph evolution, such as how fast distinct regions of the phenotype adapted to new environments and food sources associated with the fish-tetrapod transition.

Tree models and calibrations. We tested the impact on our results from various tree modelling conditions by implementing both the constant rates FBD tree model and the skyline variant SFBD²⁶, besides models including sampled ancestors

(SA) and not including them (nosa)⁵⁵. For initial analyses, all fossil calibrations (apart from the root node) were based on tip-dates only, which account for the uncertainty in the placement of fossil taxa and avoid the issue of assigning maximum age constraints that are necessary for node-based age calibrations⁶³. Additionally, we avoided biases introduced by point age calibrations on the age of the fossils by using a uniform prior distribution on the age range of the stratigraphic occurrence of the fossils.

For our focal analyses, we combine the age data from the fossil tips with that from the ichnological record to enhance our calibration procedures, as ichnofossils may place the origin of a group much earlier than the known osteological fossil record. Osteological and trace fossils may be preserved in very different sedimentary settings and, in at least some instances, fossil outcrops closest in age to the origin of a lineage may be poor in osteological remains but preserve other traces indicating the presence of a particular clade. Although rarely used, trace fossils may thus represent important calibration points for both morphological and molecular clock analyses, yielding results that would never be recovered using only tip ages or only calibration points from osteological fossil evidence. This is especially important in the case of early tetrapods considering the much older age of the ichnofossil evidence for digit-bearing tetrapods compared to the oldest known fossil tetrapod osteological data, including the oldest known tetrapod species (*Parmastega*)¹⁸. The ichnofossil data come from tetrapod trackways from Zachelmie (Poland)²⁰, dated as Eifelian, Middle Devonian—initially estimated at ~395 Ma (refs. 20,22), now estimated at ~390 Ma (refs. 13,21)—thus being ~18 Myr older than *Parmastega* and, in fact, older than most early tetrapodomorph fossils.

In all initial analyses (Results), *Tiktaalik* was recovered as the sister taxon to Tetrapoda, indicating the oldest possible stem tetrapods could have evolved at any point between that split and *Parmastega*. Therefore, our node age constraint parameterizes the age for the split between *Tiktaalik* and Total Group Tetrapoda (node representing the most recent common ancestor (MRCA) of *Tiktaalik* and tetrapods; MRCA_T). We sampled the age of the MRCA_T from an offset exponential distribution with the minimum age set to the age of the Zachelmie trackways (min MRCA_T = 390 Ma) and with the mean 8 Myr older than the tracks age (= 398 Ma), on the basis of previous estimates²².

Convergence of independent runs was assessed using average standard deviation of split frequencies (~0.01), potential scale reduction factors (~1 for all parameters) and effective sample size for each parameter greater than 200 and analysed using Tracer v.1.7.1 (ref. 64) and the RWTY package for R (ref. 65). Analyses were conducted using the CIPRES Science Gateway v.3.3 (ref. 66).

Morphological clock partitioning. Morphological data partitioning (especially clock partitioning) is almost never applied to empirical datasets. Rare exceptions include morphological clock partitioning of exceptionally large morphological datasets, including thousands of characters, which are less prone to model overfitting⁶⁷, and one much smaller dataset⁶⁸, both suggesting that divergence times and convergencies between independent runs may be negatively impacted by multiple morphological clocks. However, using strongly informative priors on the age of the root or constraining the tree topology can avoid such biases²⁷ and the exact impact of morphological clock partitioning is likely to be dataset dependent. Additionally, the implementation of separate clocks for each morphological partition has the potential to yield detailed macroevolutionary estimates across distinct regions of the phenotype^{27,59}.

For the present dataset, partitioning morphological data by anatomical or functional regions is limited by the fact that the pectoral girdle of tetrapodomorphs is an integral component of the cephalic region (as in other early vertebrates), whereas in elopistostegalians those elements become functionally distinct from the head, eventually acquiring the quite distinct locomotory morphological and functional attributes they possess in tetrapods^{11–13,68}. Therefore, to objectively identify the best-possible subdivision of the morphological characters in early tetrapodomorphs, we implemented a protocol for calculating pairwise distances between characters and subsequently testing partitioning schemes by means of clustering methods and ordination methods.

Automatically subdividing the phenotype into morphological partitions for phylogenetic inference on the basis of distance matrices and clustering methods has been previously suggested and implemented^{69,70}. The latter used the commonly implemented Euclidean distances to create a character–character distance matrix, upon which a principal coordinate analysis (PCoA, or metric multidimensional scaling) was performed to detect character clusters to define morphological partitions⁶⁹ or used K-means for cluster identification⁷⁰. However, Euclidean distances are extremely sensitive to missing data and alternative choices, such as Gower distances, provide more suitable alternatives for the handling of missing data^{71,72}. This issue creates a subsequent problem for estimating clusters using K-means, perhaps the most popular clustering approach, as it depends on an Euclidean-based distance matrix. Further, K-means are based on measuring the distance between samples and cluster centroids (that is, the centre of mass or mean vector of the cluster). The mean vector is particularly sensitive to outliers (as any other mean estimate)⁷³, which can be particularly problematic for small-sized clusters or clusters of drastically different sizes, which are to be expected from most standard-sized morphological datasets. Those limitations from Euclidean distances and K-means thus limit the ability of clustering analyses based on such approaches.

To avoid those limitations, we used Gower distances to create the intercharacter distance matrix ‘D’. For the clustering analysis, we used here an alternative solution based on partitioning around medoids (PAM, or K-medoids), which can estimate clusters using Gower distances. Most importantly, PAM is analogous to K-means but it has its clusters centred around medoids instead of centred around centroids, which are less prone to the impact from outliers and heterogeneous cluster sizes^{3,74}.

To define how many clusters the data could be partitioned into, we tested various PAM partitioning schemes ranging from the minimum number of possible partitions ($K = 2$) and a large number of partitions (that would almost certainly create overparameterization issues for the present dataset; $K = 10$). We assessed the quality of each clustering scheme using the silhouette index (Si) approach⁷⁵, which determines how well an object falls within their cluster compared to other clusters. Our results indicated the best clustering scheme to be composed of $K = 3$, closely followed by $K = 2$ partitions (Supplementary Table 3).

For further and independently testing the quality of the chosen partitioning scheme above, we used a graphic visualization approach based on t -distributed Stochastic Neighbor Embedding (t -SNE)⁷⁶. This has become a popular ordination and visualization tool in machine learning given its ability to reduce an exceptionally large number of dimensions into only two or three dimensions. More traditional ordination procedures, such as principal components analysis (PCA) and PCoA, preserve the linear relationship between datapoints at a lower dimensionality. However, as those metrics try to preserve the local distances between datapoints they become less efficient at characterizing the overall structure of high-dimensional data—it is more important to reduce the local linear distance between similar (neighbouring) datapoints while maximizing the distance between distant datapoints⁷⁶. For such cases, nonlinear ordination procedures are preferred to observe the overall data structure in a reduced number of dimensions. t -SNE has been demonstrated to be more efficient at preserving both local and global structures when reducing high-dimensional data into only two or three dimensions compared to other nonlinear ordination procedures⁷⁷, thus offering an important advantage over previously used graphic approaches to determine morphological clusters such as PCoA. The resulting clustering scheme using t -SNE finds a clear distinction between the three partitions proposed by the PAM + Si procedure (Extended Data Fig. 7), thus offering an additional support for this clustering scheme and protocol.

A technique widely familiar to evolutionary biologists is the use of Bayes factors (BF) in assessing model fit to the data in Bayesian phylogenetics⁶². BF also formed the basis of our model comparison among distinct probability distributions governing rate variation among characters and different clock models (see above). However, we did not implement BF towards estimating the quality of distinct cluster sizes or character association to distinct partitions. As previously argued^{26,27,63}, when models differ by many parameters or have different dimensionalities—that is, different tree models (for example, variations on the FBD model and sampling strategies) or, as in our case here, several candidate partition models, each with their own character dimensions and final number of partitions—they will represent the simultaneous change of several parameters that make model performance comparison extremely more complex in a manner that may not be fully captured by comparing marginal model likelihoods alone. Therefore, theory suggests that the multivariate statistical approaches taken herein (for example, PAM and t -SNE) provide more appropriate tests for partitioning schemes.

The limitations of BF towards non-equivalent multidimensional model assessment also impact a previous proposition of using character homoplasy of

characters towards inferring morphological clusters for phylogenetics⁷⁸, as it was evaluated using BF. Additionally, the character homoplasy index approach requires a maximum parsimony tree to be estimated a priori, which violates our goal of using a statistical method independent of previous phylogenetic assumptions to construct morphological partitioning schemes.

The final partitioning scheme has one partition composed exclusively of cranial characters—in the sense of cranial as in the anatomy of ‘fish-like’ tetrapodomorphs, which compose most of the dataset (Cranial 1 partition); one partition composed mostly of postcranial characters (Postcranial partition); a third partition also composed entirely by cranial characters (Cranial 2 partition) but with only one-third of the number of characters found for cranial 1 (Supplementary Table 4 gives a list of characters for each partition). Characters usually associated with the postcranium in tetrapods (for example, cleithrum) but part of the cranial anatomy of ‘fish-like’ early tetrapodomorphs, include: 24, 25, 49, 50, 99, 110–113 and 170 (for Cranial 1); and 48, 100 and 165 (for Cranial 2). All postcranial characters were found in a single partition along with a few cranial characters that change concomitantly with the postcranium and thus were clustered with them: 4, 27, 28, 33, 34, 35, 37, 38, 60, 105, 151 and 157.

R scripts for all the statistical procedures in this method are provided online (Data availability).

Strength of selection. We measured the strength of selection by comparing the variation of evolutionary rates relative to the base of the clock rate (background rate) of evolution for every tree branch (Δv) compared to the background rate of evolution (Δb), forming the rate scalar ratio ($r = \Delta v / \Delta b$), as defined by ref. ⁴². This measure is equivalent to the interpretation of relative rates of character evolution produced by relaxed Bayesian inference, in which estimates >1 indicate accelerating rates of evolution whereas <1 indicate decreasing rates of evolution^{42,79}. When rates are significantly accelerated, it provides support for positive phenotypic selection in analogy with the d_N/d_S ratio in molecular evolution, whereas strongly decelerating rates represent an instance of stabilizing selection, stasis or constraint^{42,43}.

In its original form, when evolutionary rates are at least twice as fast as the background rates ($r > 2$) that would be interpreted as a positive phenotypic selection⁴². Here, we use a different threshold, taking into account the dispersion of the distribution for the background rates. When the mean rate of evolution on a branch is greater than the background rate plus one standard deviation ($\Delta v > \mu_{\Delta b} + \sigma$) it is interpreted as an instance of positive selection. When the mean rate of evolution on a branch is less than the main background rate minus one standard deviation ($\Delta v > \mu_{\Delta b} - \sigma$) it is interpreted as an instance of stabilizing selection or stasis. R scripts for these analyses are provided online (Code availability).

Tetrapodomorph palaeoenvironments. To assess whether the fossil record of early tetrapodomorphs and dipnomorphans is potentially biased towards specific environments and strongly impacting fossil preservation rates, we surveyed the palaeoenvironment of all specimen occurrences for all taxa included in this study. Taxonomic occurrences and their respective paleoenvironments were obtained from the Paleobiology Database (<https://paleobiodb.org/>) and complemented with additional data from the literature. The results of this meta-analysis (Supplementary Table 11) shows that our taxonomic sample includes species found in a wide variety of terrestrial and marine environments, including lacustrine, fluvial, estuary, lagoonal, nearshore marine and offshore marine, among others. All environments are represented under similar frequencies, with nearly half coming from marine environments and the other half from continental aquatic environments. This suggests no particular preservation bias towards a specific environment in the early tetrapodomorph fossil record.

Statistical analysis. We performed pairwise statistical tests across time bins and analytical approaches (tip versus tip + node dating) to assess whether particular time intervals or analyses differ significantly on the posterior estimates for macroevolution parameters (for example, net diversification, turnover and relative fossilization). We assessed the normality of the distribution for each time bin using the Shapiro–Wilk normality test and visual assessment of data distribution. Additionally, we used the Bartlett test of homogeneity of variances to assess homoscedasticity in the data. All data passed those tests, so we performed pairwise t -tests among groups (Supplementary Tables 7 and 9). However, visual inspection revealed the presence of some extreme outliers for some estimates (for example, posterior sample of relative extinction estimates) and so we also conducted non-parametric pairwise Wilcoxon rank sum (Mann–Whitney) tests, which had fairly similar results to the pairwise t -tests (Supplementary Tables 9 and 10). R scripts for statistical analyses are provided online (Code availability).

Reporting Summary. Further information on research design is available in the Nature Research Reporting Summary linked to this article.

Data availability

All data generated and analysed are available online as Supplementary Data 1–3 at Harvard’s Dataverse Repository <https://doi.org/10.7910/DVN/NNVTTD>⁸⁰. Source data are provided with this paper.

Code availability

All R scripts, MrBayes command blocks and BEAST2 XML files are freely available online at Harvard's Dataverse Repository <https://doi.org/10.7910/DVN/NNVTTD>⁸⁰. R scripts for all protocols are also available on GitHub: https://github.com/tiago-simoes/MorphoEvol_Tetrapods.git.

Received: 13 January 2021; Accepted: 9 July 2021;
Published online: 23 August 2021

References

1. Simpson, G. G. *The Major Features of Evolution* (Columbia Univ. Press, 1953).
2. Gould, S. J. *The Structure of Evolutionary Theory* (Harvard Univ. Press, 2002).
3. Erwin, D. H. Novelty and innovation in the history of life. *Curr. Biol.* **25**, R930–R940 (2015).
4. Lee, M. S. Y., Cau, A., Naish, D. & Dyke, G. J. Sustained miniaturization and anatomical innovation in the dinosaurian ancestors of birds. *Science* **345**, 562–566 (2014).
5. Simões, T. R., Vernygora, O. V., Caldwell, M. W. & Pierce, S. E. Megaevolutionary dynamics and the timing of evolutionary innovation in reptiles. *Nat. Commun.* **11**, 3322 (2020).
6. Lepage, D. Avibase—the world bird database. <http://avibase.bsc-eoc.org/avibase.jsp> (Accessed 15 February 2021).
7. Uetz, P., Freed, P., Aguilar, R. & Hošek, J. The Reptile Database. <http://www.reptile-database.org> (Accessed 15 February 2021).
8. AmphibiaWeb, University of California, Berkeley, CA, USA <https://amphibiaweb.org> (Accessed 15 February 2021).
9. Mammal Diversity Database (Version 1.2). American Society of Mammalogists 10.5281/zenodo.4139818 (Accessed 15 February 2021).
10. Shubin, N. *Your Inner Fish: A Journey Into the 3.5-Billion-Year History of the Human Body* (Vintage Books, 2008).
11. Clack, J. A. The fin to limb transition: new data, interpretations, and hypotheses from paleontology and developmental biology. *Annu. Rev. Earth Planet. Sci.* **37**, 163–179 (2009).
12. Clack, J. A. *Gaining Ground: The Origin and Evolution of Tetrapods* (Indiana Univ. Press, 2012).
13. Ahlberg, P. E. Follow the footprints and mind the gaps: a new look at the origin of tetrapods. *Earth Env. Sci. Trans. R. Soc. Edinb.* **109**, 115–137 (2018).
14. Daeschler, E. B., Shubin, N. H. & Jenkins, F. A. Jr A Devonian tetrapod-like fish and the evolution of the tetrapod body plan. *Nature* **440**, 757 (2006).
15. Anderson, P. S. L., Friedman, M. & Ruta, M. Late to the table: diversification of tetrapod mandibular biomechanics lagged behind the evolution of terrestriality. *Integr. Comp. Biol.* **53**, 197–208 (2013).
16. Ruta, M., Krieger, J., Angielczyk, K. D. & Wills, M. A. The evolution of the tetrapod humerus: morphometrics, disparity, and evolutionary rates. *Earth Env. Sci. Trans. R. Soc. Edinb.* **109**, 1–19 (2018).
17. Ahlberg, P. E. *Elginerpeton pancheni* and the earliest tetrapod clade. *Nature* **373**, 420–425 (1995).
18. Beznosov, P. A., Clack, J. A., Lukševičs, E., Ruta, M. & Ahlberg, P. E. Morphology of the earliest reconstructable tetrapod *Parmastega aelidae*. *Nature* **574**, 527–531 (2019).
19. Clément, G. & Lebedev, O. Revision of the early tetrapod *Obruchevichthys vorobyeva*, 1977 from the Frasnian (Upper Devonian) of the North-western East European Platform. *Paleontol. J.* **48**, 1082–1091 (2014).
20. Niedźwiedzki, G., Szrek, P., Narkiewicz, K., Narkiewicz, M. & Ahlberg, P. E. Tetrapod trackways from the early Middle Devonian period of Poland. *Nature* **463**, 43–48 (2010).
21. Qvarnström, M., Szrek, P., Ahlberg, P. E. & Niedźwiedzki, G. Non-marine palaeoenvironment associated to the earliest tetrapod tracks. *Sci. Rep.* **8**, 1–10 (2018).
22. Friedman, M. & Brazeau, M. D. Sequences, stratigraphy and scenarios: what can we say about the fossil record of the earliest tetrapods? *Proc. R. Soc. Lond. B* **278**, 432–439 (2011).
23. Ronquist, F., Lartillot, N. & Phillips, M. J. Closing the gap between rocks and clocks using total-evidence dating. *Philos. Trans. R. Soc. B* **371**, 20150136 (2016).
24. Cloutier, R. et al. *Elpistostege* and the origin of the vertebrate hand. *Nature* **579**, 549–554 (2020).
25. Barido-Sottani, J., Aguirre-Fernández, G., Hopkins, M. J., Stadler, T. & Warnock, R. Ignoring stratigraphic age uncertainty leads to erroneous estimates of species divergence times under the fossilized birth-death process. *Proc. R. Soc. Lond. B* **286**, 20190685 (2019).
26. Zhang, C., Stadler, T., Klopstein, S., Heath, T. A. & Ronquist, F. Total-evidence dating under the fossilized birth-death process. *Syst. Biol.* **65**, 228–249 (2016).
27. Simões, T. R., Caldwell, M. W. & Pierce, S. E. Sphenodontian phylogeny and the impact of model choice in Bayesian morphological clock estimates of divergence times and evolutionary rates. *BMC Biol.* **18**, 191 (2020).
28. Zhu, M., Ahlberg, P. E., Zhao, W.-J. & Jia, L.-T. A Devonian tetrapod-like fish reveals substantial parallelism in stem tetrapod evolution. *Nat. Ecol. Evol.* **1**, 1470–1476 (2017).
29. Lu, J. et al. The earliest known stem-tetrapod from the Lower Devonian of China. *Nat. Commun.* **3**, 1160 (2012).
30. Swartz, B. A marine stem-tetrapod from the Devonian of western North America. *PLoS ONE* **7**, e33683 (2012).
31. Jeffery, J. E., Storrs, G. W., Holland, T., Tabin, C. J. & Ahlberg, P. E. Unique pelvic fin in a tetrapod-like fossil fish, and the evolution of limb patterning. *Proc. Natl Acad. Sci. USA* **115**, 12005–12010 (2018).
32. Dickson, B., Clack, J. A., Smithson, T. R. & Pierce, S. E. Functional adaptive landscapes predict terrestrial capacity at the origin of limbs. *Nature* **589**, 242–245 (2020).
33. Simões, T. R., Caldwell, M. W., Palci, A. & Nydam, R. L. Giant taxon-character matrices: quality of character constructions remains critical regardless of size. *Cladistics* **33**, 198–219 (2017).
34. Brazeau, M. D. Problematic character coding methods in morphology and their effects. *Biol. J. Linn. Soc.* **104**, 489–498 (2011).
35. Sereno, P. C. Logical basis for morphological characters in phylogenetics. *Cladistics* **23**, 565–587 (2007).
36. Ronquist, F. et al. MrBayes 3.2: efficient Bayesian phylogenetic inference and model choice across a large model space. *Syst. Biol.* **61**, 539–542 (2012).
37. Bouckaert, R. et al. BEAST 2.5: an advanced software platform for Bayesian evolutionary analysis. *PLoS Comp. Biol.* **15**, e1006650 (2019).
38. King, B., Qiao, T., Lee, M. S. Y., Zhu, M. & Long, J. A. Bayesian morphological clock methods resurrect placoderm monophly and reveal rapid early evolution in jawed vertebrates. *Syst. Biol.* **66**, 499–516 (2017).
39. O'Reilly, J. E. & Donoghue, P. C. Tips and nodes are complementary not competing approaches to the calibration of molecular clocks. *Biol. Lett.* **12**, 20150975 (2016).
40. Close, R. A. et al. Diversity dynamics of Phanerozoic terrestrial tetrapods at the local-community scale. *Nat. Ecol. Evol.* **3**, 590–597 (2019).
41. Revell, L. J. phytols: an R package for phylogenetic comparative biology (and other things). *Methods Ecol. Evol.* **3**, 217–223 (2012).
42. Baker, J., Meade, A., Pagel, M. & Venditti, C. Positive phenotypic selection inferred from phylogenies. *Biol. J. Linn. Soc.* **118**, 95–115 (2016).
43. Yang, Z. *Molecular Evolution: A Statistical Approach* (Oxford Univ. Press, 2014).
44. Markey, M. J. & Marshall, C. R. Terrestrial-style feeding in a very early aquatic tetrapod is supported by evidence from experimental analysis of suture morphology. *Proc. Natl Acad. Sci. USA* **104**, 7134–7138 (2007).
45. Lemberg, J. B., Daeschler, E. B. & Shubin, N. H. The feeding system of *Tiktaalik roseae*: an intermediate between suction feeding and biting. *Proc. Natl Acad. Sci. USA* **118**, e2016421118 (2021).
46. MacIver, M. A., Schmitz, L., Mugan, U., Murphey, T. D. & Mobley, C. D. Massive increase in visual range preceded the origin of terrestrial vertebrates. *Proc. Natl Acad. Sci. USA* **114**, E2375–E2384 (2017).
47. Molnar, J., Hutchinson, J. R., Diogo, R., Clack, J. A. & Pierce, S. E. Evolution of forelimb musculoskeletal function across the fish-to-tetrapod transition. *Sci. Adv.* **7**, eabd7457 (2021).
48. Lennie, K. I., Manske, S. L., Mansky, C. F. & Anderson, J. S. Locomotory behaviour of early tetrapods from Blue Beach, Nova Scotia, revealed by novel microanatomical analysis. *R. Soc. Open Sci.* **8**, 210281 (2021).
49. Cantalapiedra, J. L., Prado, J. L., Fernández, M. H. & Alberdi, M. T. Decoupled ecomorphological evolution and diversification in Neogene-Quaternary horses. *Science* **355**, 627–630 (2017).
50. Luo, A., Duchêne, D. A., Zhang, C., Zhu, C.-D. & Ho, S. Y. W. A simulation-based evaluation of tip-dating under the fossilized birth-death process. *Syst. Biol.* **69**, 325–344 (2020).
51. Aberer, A. J., Krompass, D. & Stamatakis, A. Pruning rogue taxa improves phylogenetic accuracy: an efficient algorithm and web-service. *Syst. Biol.* **62**, 162–166 (2013).
52. Vernygora, O. V., Simões, T. R. & Campbell, E. O. Evaluating the performance of probabilistic algorithms for phylogenetic analysis of big morphological datasets: a simulation study. *Syst. Biol.* **69**, 1088–1105 (2020).
53. Wright, A., Wagner, P. J. & Wright, D. F. *Testing Character Evolution Models in Phylogenetic Paleobiology: A Case Study with Cambrian Echinoderms* (Cambridge Univ. Press, 2021).
54. Heath, T. A., Huelsenbeck, J. P. & Stadler, T. The fossilized birth-death process for coherent calibration of divergence-time estimates. *Proc. Natl Acad. Sci. USA* **111**, 2957–2966 (2014).
55. Gavryushkina, A., Welch, D., Stadler, T. & Drummond, A. J. Bayesian inference of sampled ancestor trees for epidemiology and fossil calibration. *PLoS Comput. Biol.* **10**, e1003919 (2014).
56. Warnock, R. C. M., Heath, T. A. & Stadler, T. Assessing the impact of incomplete species sampling on estimates of speciation and extinction rates. *Paleobiology* **46**, 137–157 (2020).

57. Ho, S. Y., Phillips, M. J., Drummond, A. J. & Cooper, A. Accuracy of rate estimation using relaxed-clock models with a critical focus on the early metazoan radiation. *Mol. Biol. Evol.* **22**, 1355–1363 (2005).
58. Bapst, D. W., Wright, A. M., Matzke, N. J. & Lloyd, G. T. Topology, divergence dates, and macroevolutionary inferences vary between different tip-dating approaches applied to fossil theropods (Dinosauria). *Biol. Lett.* **12**, 20160237 (2016).
59. Paterson, J. R., Edgecombe, G. D. & Lee, M. S. Y. Trilobite evolutionary rates constrain the duration of the Cambrian explosion. *Proc. Natl Acad. Sci. USA* **116**, 4394–4399 (2019).
60. Zhang, C. & Wang, M. Bayesian tip dating reveals heterogeneous morphological clocks in Mesozoic birds. *R. Soc. Open Sci.* **6**, 182062 (2019).
61. Xie, W., Lewis, P. O., Fan, Y., Kuo, L. & Chen, M.-H. Improving marginal likelihood estimation for Bayesian phylogenetic model selection. *Syst. Biol.* **60**, 150–160 (2011).
62. Nylander, J. A. A., Ronquist, F., Huelsenbeck, J. P. & Nieves-Aldrey, J. Bayesian phylogenetic analysis of combined data. *Syst. Biol.* **53**, 47–67 (2004).
63. Ronquist, F. et al. A total-evidence approach to dating with fossils, applied to the early radiation of the Hymenoptera. *Syst. Biol.* **61**, 973–999 (2012).
64. Rambaut, A., Suchard, M. A., Xie, D. & Drummond, A. J. *Tracer v1.7* <http://beast.bio.ed.ac.uk/Tracer> (2018).
65. Warren, D. L., Geneva, A. J. & Lanfear, R. RWTY (R We There Yet): an R package for examining convergence of Bayesian phylogenetic analyses. *Mol. Biol. Evol.* **34**, 1016–1020 (2017).
66. Miller, M. A., Pfeiffer, W. & Schwartz, T. Creating the CIPRES Science Gateway for inference of large phylogenetic trees. In *Gateway Computing Environments Workshop (GCE)* (IEEE, 2010).
67. Lee, M. S. Y. Multiple morphological clocks and total-evidence tip-dating in mammals. *Biol. Lett.* **12**, 20160033 (2016).
68. Long, J. A. & Gordon, M. S. The greatest step in vertebrate history: a paleobiological review of the fish-tetrapod transition. *Physiol. Biochem. Zool.* **77**, 700–719 (2004).
69. Goswami, A. & Polly, P. D. in *Carnivoran Evolution: New Views on Phylogeny, Form and Function* (eds Goswami, A. & Friscia, A.) 141–164 (Cambridge Univ. Press, 2010).
70. Lanfear, R., Frandsen, P. B., Wright, A. M., Senfeld, T. & Calcott, B. PartitionFinder 2: new methods for selecting partitioned models of evolution for molecular and morphological phylogenetic analyses. *Mol. Biol. Evol.* **34**, 772–773 (2017).
71. Lloyd, G. T. Estimating morphological diversity and tempo with discrete character–taxon matrices: implementation, challenges, progress, and future directions. *Biol. J. Linn. Soc.* **118**, 131–151 (2016).
72. Lehmann, O. E. R., Ezcurra, M. D., Butler, R. J. & Lloyd, G. T. Biases with the Generalized Euclidean Distance measure in disparity analyses with high levels of missing data. *Palaeontology* **62**, 837–849 (2019).
73. Rencher, A. C. & Christensen, W. F. *Methods of Multivariate Analysis* (John Wiley & Sons, 2012).
74. Budiaji, W. & Leisch, F. Simple K-medoids partitioning algorithm for mixed variable data. *Algorithms* **12**, 177 (2019).
75. Rousseeuw, P. J. Silhouettes: a graphical aid to the interpretation and validation of cluster analysis. *J. Comp. Appl. Math.* **20**, 53–65 (1987).
76. Van Der Maaten, L. & Hinton, G. Visualizing data using t-SNE. *J. Mach. Learn. Res.* **9**, 2579–2605 (2008).
77. Van Der Maaten, L. Learning a parametric embedding by preserving local structure. *Proc. Machine Learn. Res.* **5**, 384–391 (2009).
78. Rosa, B. B., Melo, G. A. & Barbeitos, M. S. Homoplasy-based partitioning outperforms alternatives in Bayesian analysis of discrete morphological data. *Syst. Biol.* **68**, 657–671 (2019).
79. Ronquist, F., Huelsenbeck, J., Teslenko, M. & Nylander, J. A. A. *MrBayes version 3.2 Manual: Tutorials and Model Summaries* <https://nbisweden.github.io/MrBayes/manual.html> (2019).
80. Simoes, T. R. & Pierce, S. E. *Supplementary Data 1–4 for “Sustained High Rates of Morphological Evolution During the Rise of Tetrapods”* <https://doi.org/10.7910/DVN/NNVTTD> (Harvard Dataverse, 2021).

Acknowledgements

We thank C. Zhang for discussions and J. Barido-Sottani for valuable assistance with the treeWoffset operator of BEAST2. We also thank M. Caldwell and K. Jones for comments on an earlier version of the manuscript. T.R.S. was supported by an Alexander Agassiz postdoctoral fellowship (Museum of Comparative Zoology, Harvard University) and a National Sciences and Engineering Council of Canada (NSERC) postdoctoral fellowship. Additional funds were provided by Harvard University to S.E.P.

Author contributions

T.R.S. and S.E.P. conceived and designed the project. T.R.S. updated the morphological dataset, conducted phylogenetic and statistical analyses, interpreted the data and wrote the manuscript. S.E.P. updated the morphological dataset, interpreted the data and wrote the manuscript.

Competing interests

The authors declare no competing interests.

Additional information

Extended data is available for this paper at <https://doi.org/10.1038/s41559-021-01532-x>.

Supplementary information The online version contains supplementary material available at <https://doi.org/10.1038/s41559-021-01532-x>.

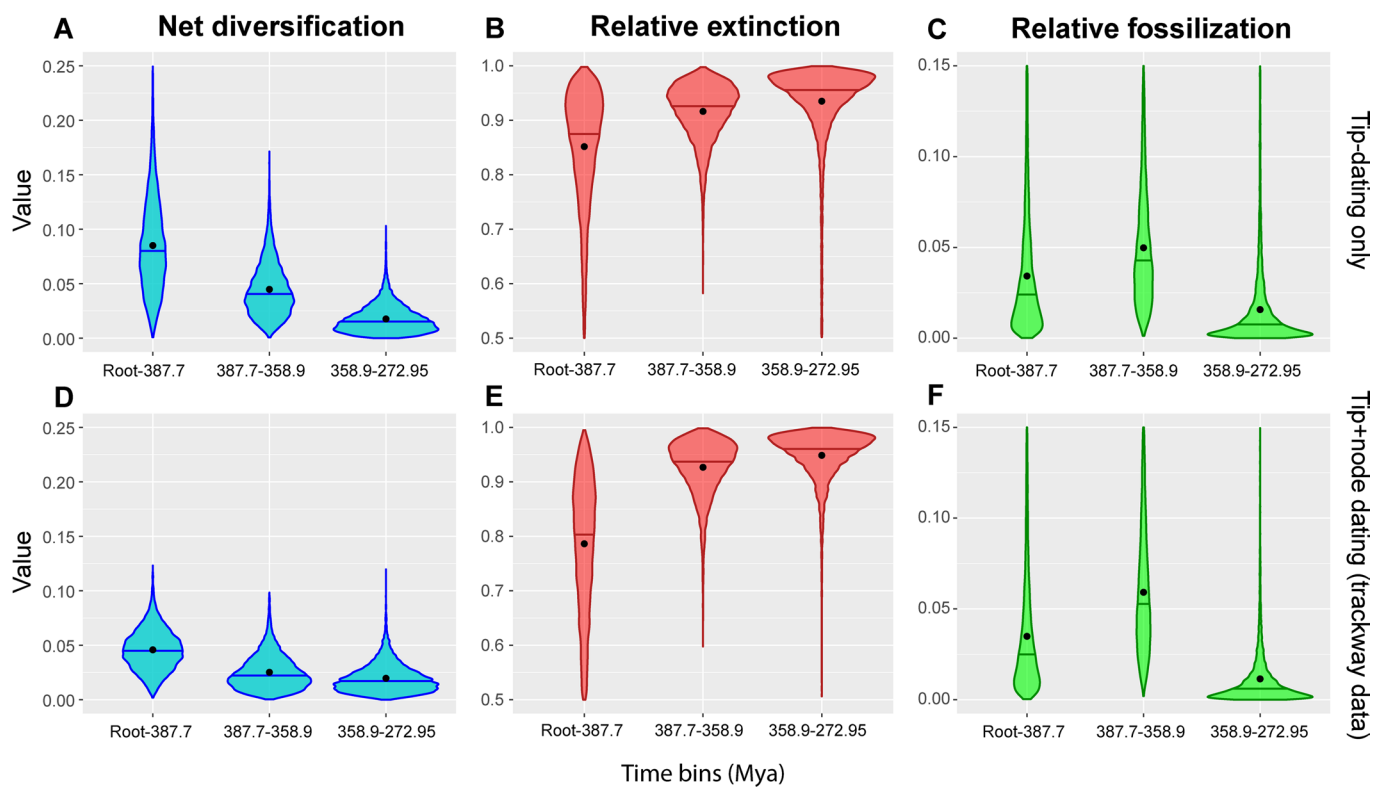
Correspondence and requests for materials should be addressed to T.R.S.

Peer review information *Nature Ecology & Evolution* thanks Neil Brocklehurst and the other, anonymous, reviewer(s) for their contribution to the peer review of this work. Peer review reports are available.

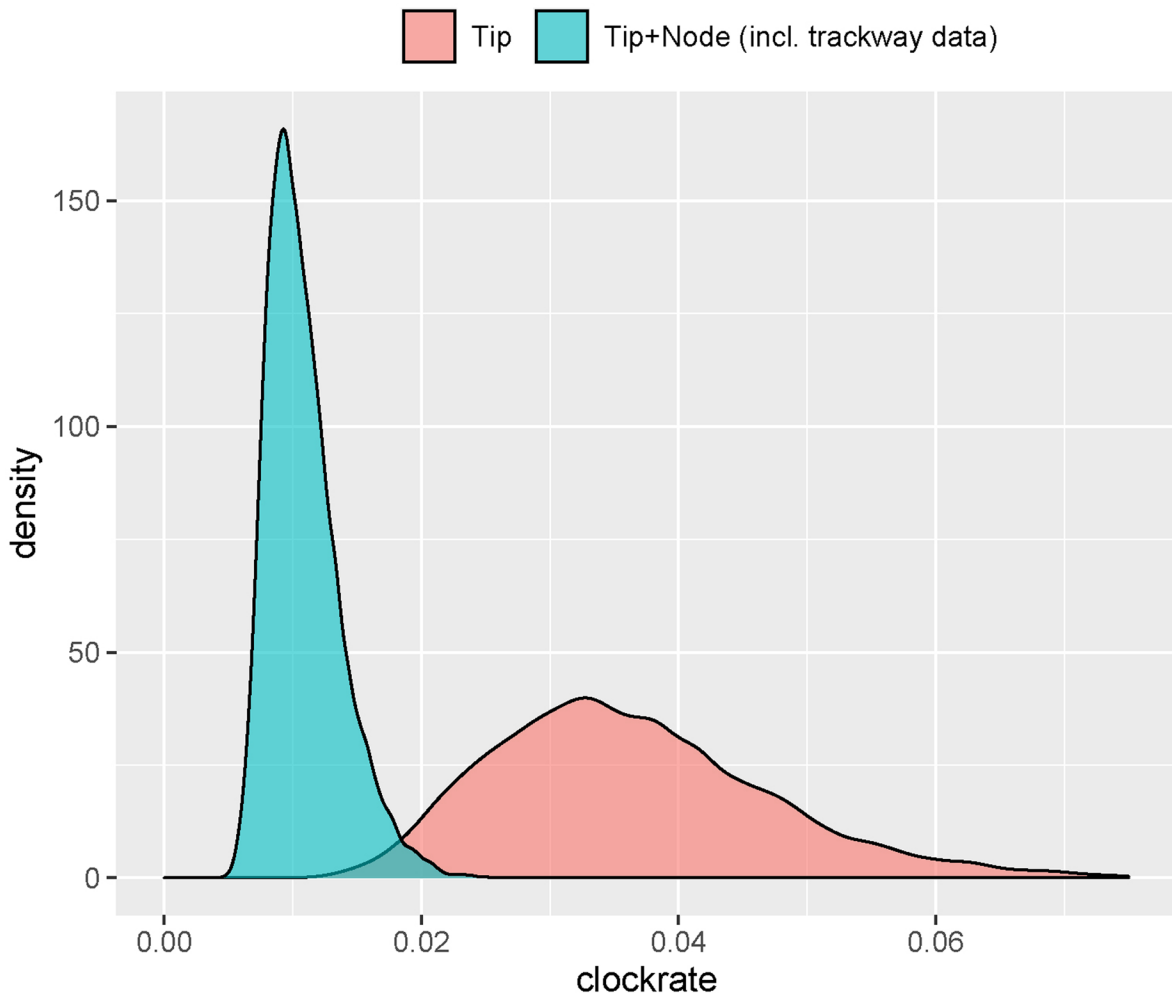
Reprints and permissions information is available at www.nature.com/reprints.

Publisher's note Springer Nature remains neutral with regard to jurisdictional claims in published maps and institutional affiliations.

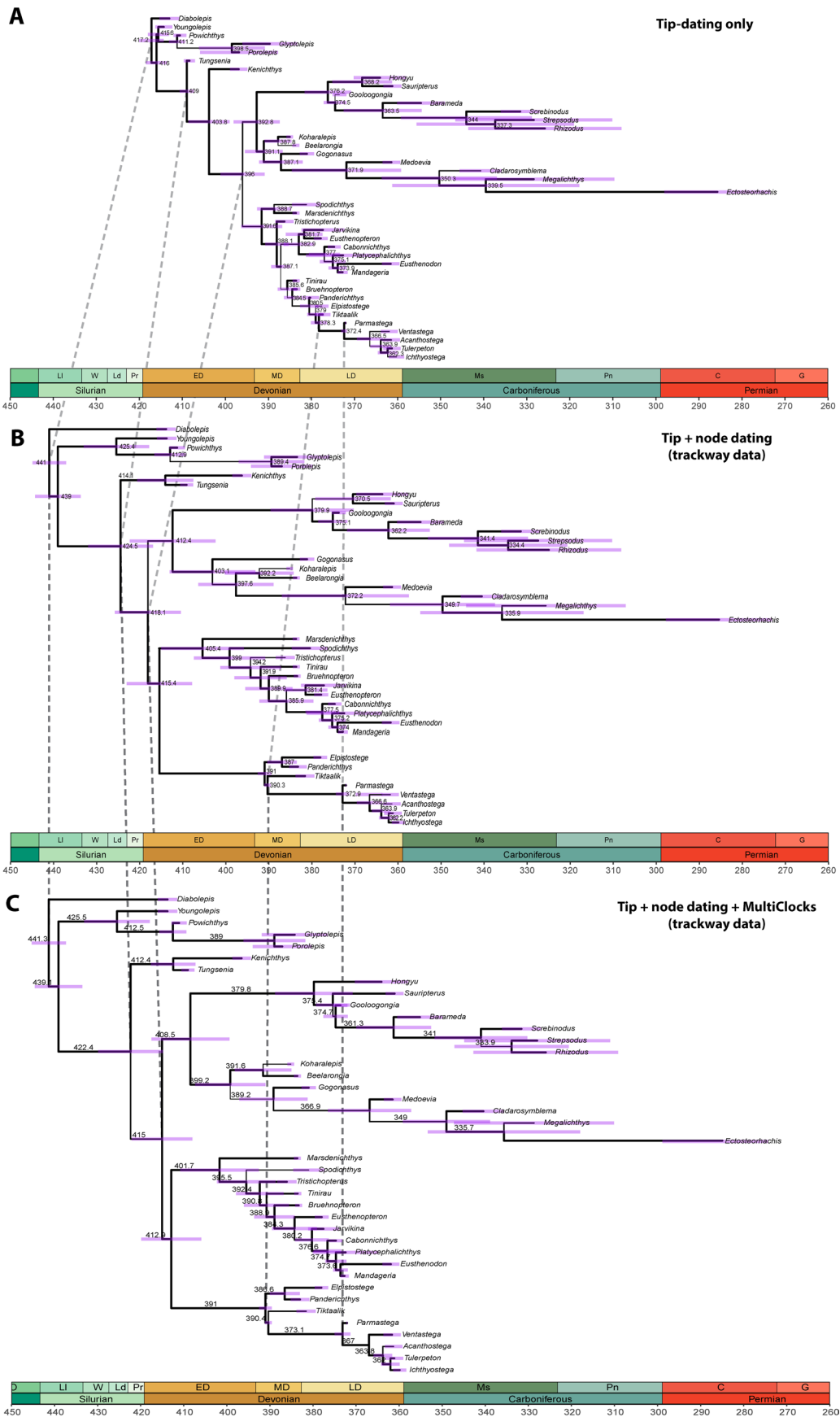
© The Author(s), under exclusive licence to Springer Nature Limited 2021



Extended Data Fig. 1 | Violin plots for estimates from SFBD free parameters across time bins. **a**, violin plots from main tip-dating only analysis. **b**, violin plots after incorporating the age of the Zachełmie tracks. Net diversification nearly halves for the first and second time bins using the new divergence times. Relative extinction values also decrease but, to a lower extent, whereas median relative fossilization remains similar between analyses (see also Fig. 2). However, the new diversification scenario (B) suggests a less drastic reduction in net diversification values across time bins during early tetrapodomorph evolution.



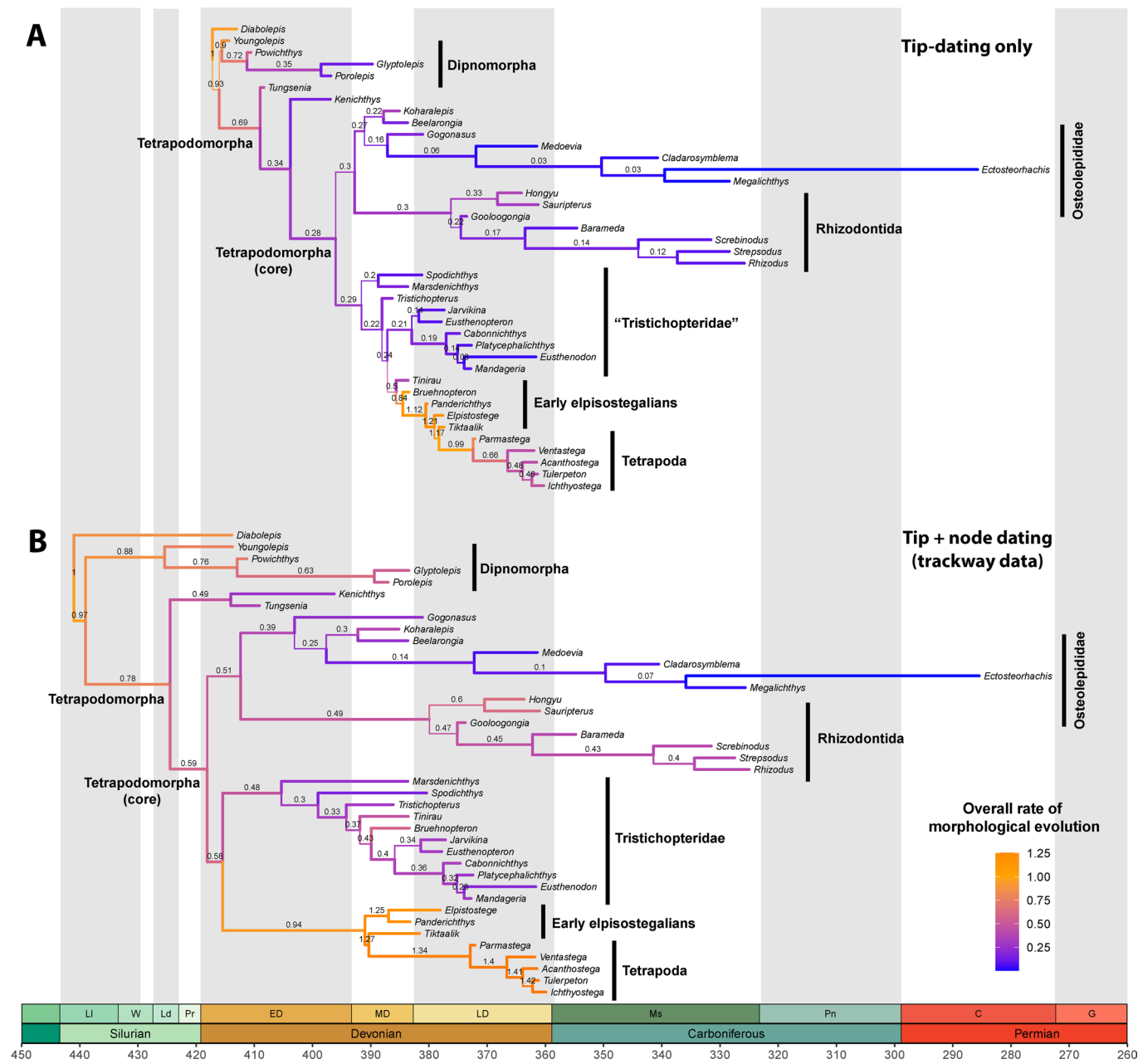
Extended Data Fig. 2 | Kernel density plot for the base of the clock rate among different calibration strategies. Results for the main tip-dating analysis using the SFBD tree model (see also Supplementary Fig. 12, 13) and results from the main tip+node dating analysis (including trackway data) using the SFBD tree model (see also Supplementary Figs. 16, 17), with medians = 0.01083 vs 0.03514, respectively.



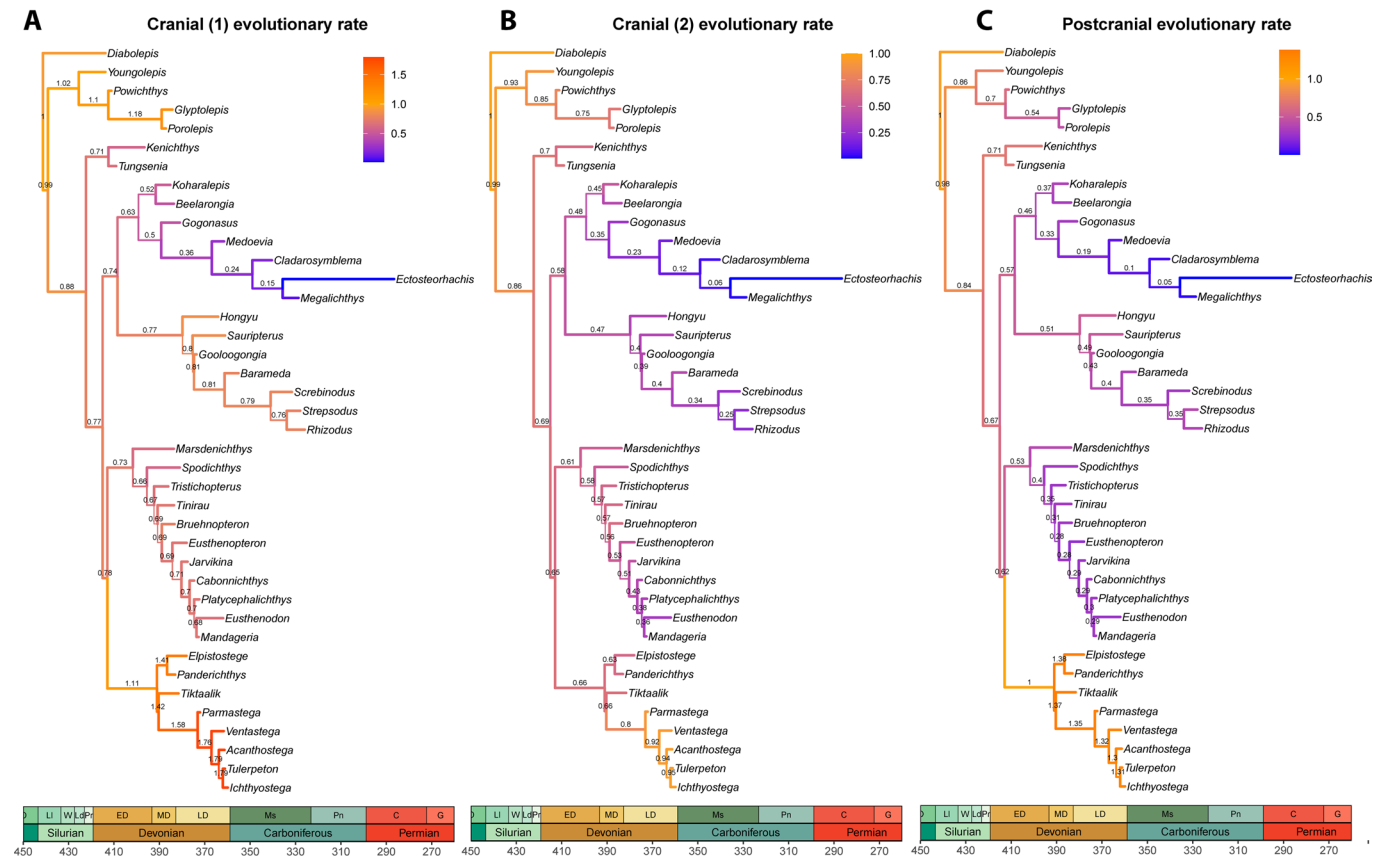
Extended Data Fig. 3 | See next page for caption.

Extended Data Fig. 3 | Comparison of divergence time and MCT topologies obtained across distinct analyses using distinct calibration strategies.

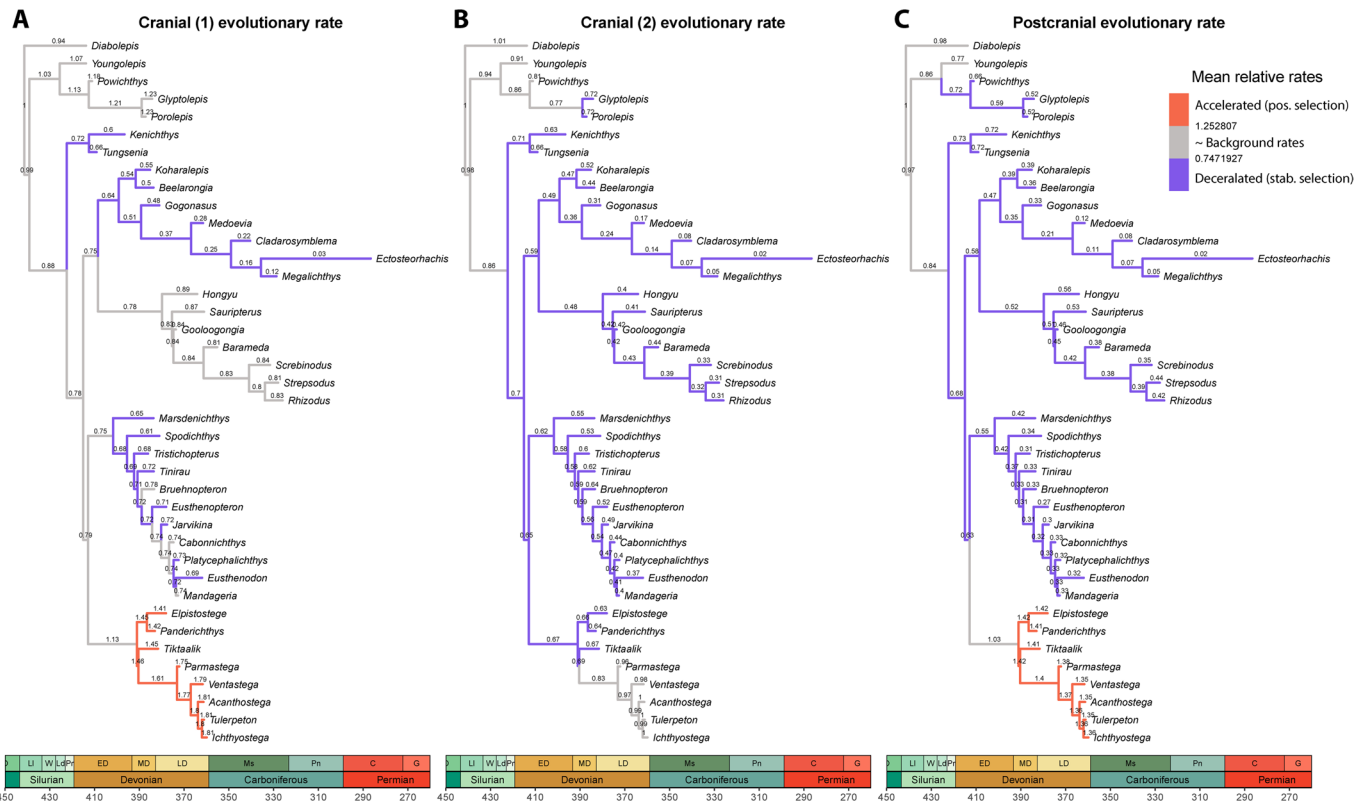
a, results from the main tip-dating analysis using the SFBD tree model (see also Supplementary Information Figs. 12, 13). **b**, results from the main tip+node dating analysis (including trackway data) using the SFBD tree model (see also Supplementary Information Figs. 16, 17). **c**, Results from the main tip+node dating analysis (including trackway data) using partitioned morphological clocks (see also Supplementary Information Figs. 18, 19). Node values represent median ages and purple error bars represent the 95% highest posterior density (HPD) intervals.



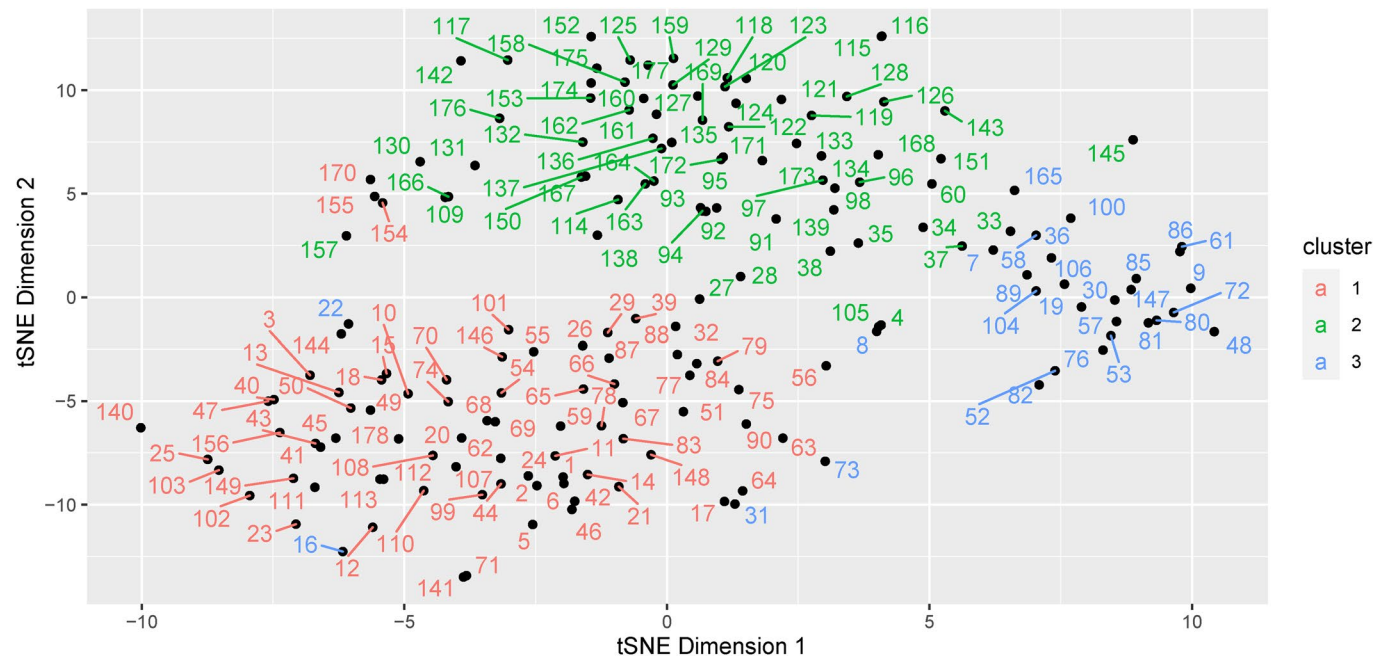
Extended Data Fig. 4 | Overall relative rates of morphological evolution in early tetrapodomorphs using distinct calibration strategies. **a**, rates of morphological evolution obtained from the main tip-dating only analysis. **b**, overall relative rates of morphological evolution obtained from the main tip+node dating analysis (including trackway age data) using a single clock partition. Under the new evolutionary scenario, (b) estimated rates of morphological evolution within Elpistostegaliens are closer in magnitude to evolutionary rates in other clades in the tree. However, as the branches leading up to other tetrapodomorph lineages also become somewhat proportionally longer chronologically, Elpistostegaliens still retained the highest relative rates of morphological evolution in the entire tree.



Extended Data Fig. 5 | Relative rates of morphological evolution using partitioned morphological clocks. Models and calibration parameters as in Extended Data Fig. 4b.

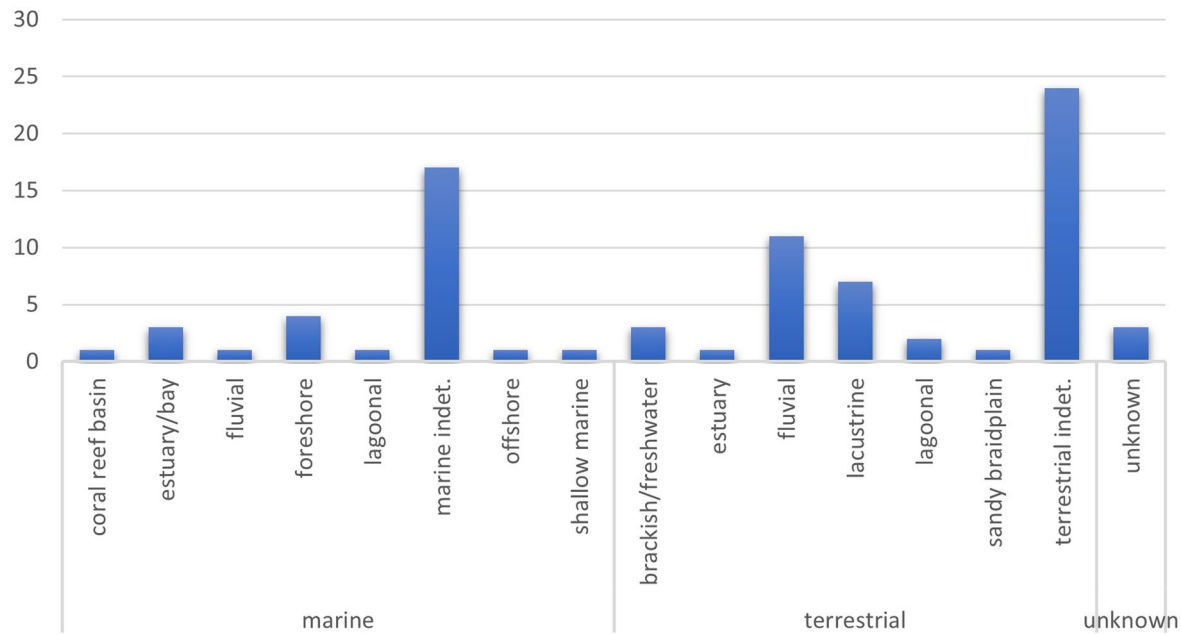


Extended Data Fig. 6 | Display of significantly accelerating or decelerating rates of evolution across lineages. Relative rates of morphological evolution using the same models and calibrations as in Extended Data Fig. 4b but using partitioned morphological clocks. Branch colouring indicates whether rates are significantly higher (> 1.297040 , in red) or lower (< 0.735828 , in blue) by one standard deviation from the background rate ($=1.0$). Grey branches indicate rates are not significantly different from background rates.



Extended Data Fig. 7 | Nonlinear multidimensional scaling analysis using t-SNE plotted with morphological character clusters identified by the PAM+Si method highlighted in different colours. Numbers indicate character numbers in the updated character list available as Supplementary Data 1.

Count of species by depositional environment



Extended Data Fig. 8 | Histograms of depositional paleo-environment of all occurrences of all dipnomorphans and early tetrapodomorphs taxa assessed here. Data obtained from the Paleobiology Database and from literature survey. For raw data, see Dataset S3.

Reporting Summary

Nature Portfolio wishes to improve the reproducibility of the work that we publish. This form provides structure for consistency and transparency in reporting. For further information on Nature Portfolio policies, see our [Editorial Policies](#) and the [Editorial Policy Checklist](#).

Statistics

For all statistical analyses, confirm that the following items are present in the figure legend, table legend, main text, or Methods section.

n/a Confirmed

- The exact sample size (n) for each experimental group/condition, given as a discrete number and unit of measurement
- A statement on whether measurements were taken from distinct samples or whether the same sample was measured repeatedly
- The statistical test(s) used AND whether they are one- or two-sided
Only common tests should be described solely by name; describe more complex techniques in the Methods section.
- A description of all covariates tested
- A description of any assumptions or corrections, such as tests of normality and adjustment for multiple comparisons
- A full description of the statistical parameters including central tendency (e.g. means) or other basic estimates (e.g. regression coefficient) AND variation (e.g. standard deviation) or associated estimates of uncertainty (e.g. confidence intervals)
- For null hypothesis testing, the test statistic (e.g. F , t , r) with confidence intervals, effect sizes, degrees of freedom and P value noted
Give P values as exact values whenever suitable.
- For Bayesian analysis, information on the choice of priors and Markov chain Monte Carlo settings
- For hierarchical and complex designs, identification of the appropriate level for tests and full reporting of outcomes
- Estimates of effect sizes (e.g. Cohen's d , Pearson's r), indicating how they were calculated

Our web collection on [statistics for biologists](#) contains articles on many of the points above.

Software and code

Policy information about [availability of computer code](#)

Data collection No software was used for data collection

Data analysis Our data was compiled in Mesquite (v. 3.04); our analysis were performed in the phylogenetic software Mr, Bayes (v. 3.2.7a) and BEAST2. Statistical analyses and graphic plots were conducted/produced in R using customized scripts. All the necessary code for phylogenetic analyses and R scripts are provided as supplementary data.

For manuscripts utilizing custom algorithms or software that are central to the research but not yet described in published literature, software must be made available to editors and reviewers. We strongly encourage code deposition in a community repository (e.g. GitHub). See the Nature Portfolio [guidelines for submitting code & software](#) for further information.

Data

Policy information about [availability of data](#)

All manuscripts must include a [data availability statement](#). This statement should provide the following information, where applicable:

- Accession codes, unique identifiers, or web links for publicly available datasets
- A description of any restrictions on data availability
- For clinical datasets or third party data, please ensure that the statement adheres to our [policy](#)

All data sets, tree files, log files and stats files are available on Harvard Dataverse (permanent link provided in the paper)

Field-specific reporting

Please select the one below that is the best fit for your research. If you are not sure, read the appropriate sections before making your selection.

Life sciences Behavioural & social sciences Ecological, evolutionary & environmental sciences

For a reference copy of the document with all sections, see nature.com/documents/nr-reporting-summary-flat.pdf

Ecological, evolutionary & environmental sciences study design

All studies must disclose on these points even when the disclosure is negative.

Study description

We conducted revisions and updates on a phylogenetic dataset on early tetrapodomorphs followed by evolutionary analyses using relaxed morphological clocks. We expanded current morphological clock implementations by providing new approaches to automatically partition for logical data and detect the strength of selection using the results of those analyses.

Research sample

The data includes discrete morphological characters obtained from 43 extinct species representing all major groups of early tetrapodomorphs, including early tetrapods. Most of the original data comes from a series of previous studies, with the latest updated information obtained from ref 24 in the main text.

Sampling strategy

See ref 24 and others therein

Data collection

See ref 24 and others therein

Timing and spatial scale

N/A

Data exclusions

No data were excluded

Reproducibility

Some of the analyses conducted were repeated multiple times, yielding similar results in terms of posterior parameter distributions.

Randomization

N/A

Blinding

Blinding was not relevant to this data set, and set of analyses.

Did the study involve field work? Yes No

Reporting for specific materials, systems and methods

We require information from authors about some types of materials, experimental systems and methods used in many studies. Here, indicate whether each material, system or method listed is relevant to your study. If you are not sure if a list item applies to your research, read the appropriate section before selecting a response.

Materials & experimental systems

n/a	Involved in the study
<input checked="" type="checkbox"/>	<input type="checkbox"/> Antibodies
<input checked="" type="checkbox"/>	<input type="checkbox"/> Eukaryotic cell lines
<input type="checkbox"/>	<input checked="" type="checkbox"/> Palaeontology and archaeology
<input checked="" type="checkbox"/>	<input type="checkbox"/> Animals and other organisms
<input checked="" type="checkbox"/>	<input type="checkbox"/> Human research participants
<input checked="" type="checkbox"/>	<input type="checkbox"/> Clinical data
<input checked="" type="checkbox"/>	<input type="checkbox"/> Dual use research of concern

Methods

n/a	Involved in the study
<input checked="" type="checkbox"/>	<input type="checkbox"/> ChIP-seq
<input checked="" type="checkbox"/>	<input type="checkbox"/> Flow cytometry
<input checked="" type="checkbox"/>	<input type="checkbox"/> MRI-based neuroimaging

Palaeontology and Archaeology

Specimen provenance

The provenance of the specimens used here is available on the supplementary information of ref 24 and others therein

Specimen deposition

All specimens were observed in publicly accessible museum and university collections across different countries.

Dating methods

No new dates were provided for individual specimens. Bayesian inferred posterior ages for each taxon is available in Supplementary Data

Tick this box to confirm that the raw and calibrated dates are available in the paper or in Supplementary Information.

Ethics oversight

No ethical approval or guidance was required for this study as all specimens included for the analyses had been previously described

Ethics oversight

and published in the literature and are deposited in publicly accessible museum collections.

Note that full information on the approval of the study protocol must also be provided in the manuscript.